

Non-linear dimension reduction in factor-augmented vector autoregressions

KARIN KLIEBER*

Oesterreichische Nationalbank

September 12, 2023

This paper introduces non-linear dimension reduction in factor-augmented vector autoregressions to analyze the effects of different economic shocks. I argue that controlling for non-linearities between a large-dimensional dataset and the latent factors is particularly useful during turbulent times of the business cycle. In simulations, I show that non-linear dimension reduction techniques yield good forecasting performance, especially when data is highly volatile. In an empirical application, I identify a monetary policy as well as an uncertainty shock excluding and including observations of the COVID-19 pandemic. Those two applications suggest that the non-linear FAVAR approaches are capable of dealing with the large outliers caused by the COVID-19 pandemic and yield reliable results in both scenarios.

JEL: C11, C32, C40, C55, E37

Keywords: Dimension reduction, machine learning, non-linear factor-augmented vector autoregression, monetary policy shock, uncertainty shock, impulse response analysis, COVID-19

*Oesterreichische Nationalbank. *Address:* Otto-Wagner-Platz 3, 1090 Vienna, Austria. *Email:* karin.klieber@oenb.at. I thank Florian Huber, Niko Hauzenberger, Michael Pfarrhofer, Anna Stelzer, Andreas Tsopanakis as well as the participants of the 2nd Workshop on High-Dimensional Data Analysis at the Universidad Carlos III de Madrid and the ICMAIF 2023 conference for valuable comments and suggestions. The views expressed in this paper do not necessarily reflect those of the Oesterreichische Nationalbank or the Eurosystem.

1 Introduction

The COVID-19 pandemic belongs to the severest health, economic and social crises in recent decades and poses the greatest challenge to the world economy since World War II. The virus has spread around the globe and paralyzed entire economic sectors and activities. For economic modeling, the COVID-19 pandemic entails dealing with huge, unprecedented outliers in datasets which adversely affect the reliability of established, mostly linear, economic models. To the detriment of those commonly used models, economic indicators and variables are prone to unanticipated movements and do not respond in the way they are supposed to. Large shifts in the level of certain variables and strong deviations from their usual paths clearly aggravate the challenge of handling large outliers within existing econometric models. As a solution, very recent studies suggest either discarding these outliers (e.g., Schorfheide and Song, 2020) or tailoring workhorse models to include COVID-19 information via priors (e.g., Lenza and Primiceri, 2020; Carriero et al., 2022b; Cascaldi-Garcia, 2022). Primiceri and Tambalotti (2020) and Ng (2021) take a structural perspective and interpret the COVID-19 pandemic as an exclusive shock to the economy. Another strategy is to incorporate highly non-linear techniques into existing models (e.g., Huber et al., 2020; Hauzenberger et al., 2022), which I also pursue in this paper.

The model introduced in this paper extends the factor-augmented vector autoregression (FAVAR) model as proposed by Bernanke et al. (2005) to a more general framework. This approach allows to flexibly model the relationship between a large number of regressors and the factors. Similar to non-linear dynamic factor models (see, e.g., Feng et al., 2018b,a; Dixon and Polson, 2019; Wang et al., 2019; Andreini et al., 2020) I assume that a small number of unobserved factors can explain the underlying dynamics of many economic and financial variables without restricting it to be linear. While the existing literature on non-linear FAVAR models mainly focuses on time variation or state dependencies in the coefficients and/or in the error variances (see, e.g., Korobilis, 2013; Ellis et al., 2014; Eickmeier et al., 2015; Huber and Fischer, 2018), this paper accounts for potential non-linear relationships between the high-dimensional dataset and its lower-dimensional factor representation. For the non-linear FAVAR, I apply non-linear dimension reduction techniques borrowed from the machine learning literature (Roweis and Saul, 2000; Heaton, 2008; Goodfellow et al., 2016) for constructing the latent factors. Recent approaches for dimension reduction non-linearly compress the information in a dataset, thereby allowing for uncovering more complex patterns in the underlying panel of economic or financial time series (see, e.g., Gallant and White, 1992; Chakraborty and Joseph, 2017; Heaton et al., 2017; Mullainathan and Spiess, 2017; Feng et al., 2018a; Kelly et al., 2018; Coulombe et al., 2019; Coulombe, 2020).

The proposed approach can be seen as a general form of the commonly used FAVAR model enriched with non-linearities in the relation between the covariates and the factors. In particular, it not only captures a high-dimensional dataset in a reduced form but nests various functional forms in the factor structure making it a powerful tool for economic analysis. In two different empirical application, I assess how controlling for non-linearities in the factor structures affects dynamic responses to economic shocks. I develop a ‘*Locally Embedded FAVAR*’ and a ‘*Deep Dynamic FAVAR*’ and compare them to the commonly used linear FAVAR. While the former uses locally linear embedding (LLE) from the manifold learning literature (Roweis and Saul,

2000), the latter can be interpreted as a modification of the deep dynamic factor model as proposed in Dixon and Polson (2019) and Andreini et al. (2020) and is based on an autoencoder.

Before I present the performance of the proposed approaches in two empirical applications, I investigate the properties of the models using artificial data. The analysis reveals that the non-linear techniques yield superior forecasting performance and controlling for non-linearities yields stable and reliable results when datasets involve large outliers similar to the ones observed during the COVID-19 pandemic.

As a next step, I consider two empirical applications based on US data. First, I identify an expansionary monetary policy shock and compare the impulse responses generated by the linear and non-linear FAVAR approaches when the sample ends in 2019 and when the pandemic observations are included. To recover the structural shocks of the models, I rely on the well established identification schemes of imposing short-run restrictions on variables that are assumed to respond with a certain delay to a cut in interest rates (see, e.g., Bernanke et al., 2005; Christiano et al., 2005; Stock and Watson, 2005; Boivin et al., 2009).

The second application imposes an uncertainty shock on the macroeconomic and financial variables of the US economy. This involves constructing an uncertainty index which I do by following Jurado et al. (2015). I identify the structural vector autoregression (SVAR) by adding the uncertainty proxy and ordering it first (see, e.g., Bloom, 2009; Koop and Korobilis, 2014; Carriero et al., 2015; Baker et al., 2016; Carriero et al., 2018, 2021). Again, this analysis is carried out for a sample that ends in 2019 and one that includes the pandemic.

Model results show that the FAVAR approaches with either linear or non-linear compression techniques yield similar impulse responses to monetary policy as well as uncertainty shocks in tranquil times. However, when I include the pandemic observations, non-linear techniques yield tighter confidence bands and provide responses in line with economic theory whereas linear models suffer from large uncertainty bands and ambiguous responses. Overall, for both shocks considered, results suggest that the non-linear FAVAR models reliably measure responses to economic shocks, especially, in turbulent times such as the COVID-19 pandemic.

The remainder of this paper is structured as follows. Section 2 presents the proposed general FAVAR model which nests a broad range of dimension reduction techniques. The identification strategies chosen to recover the structural shocks are discussed in Section 3. Section 4 applies the proposed FAVAR approaches to synthetic data. Section 5 describes the dataset, analyzes the properties of the latent factor in great detail and provides the results of the impulse response analysis for a monetary policy and an uncertainty shock before and during the COVID-19 crisis. The last section summarizes and concludes the paper.

2 A general FAVAR

Let \mathbf{D}_t denote an $N \times 1$ vector of macroeconomic and financial variables observed at time $t = 1, \dots, T$. The number of variables is large compared to the number of observations (i.e., $T \ll N$). I assume that the economy is driven by the dynamics of the variables in \mathbf{D}_t , which may feature highly non-linear dependencies, and that those dynamics can be captured in a small, Q -dimensional set of latent factors \mathbf{F}_t . In the following, the observation equation of the model

is given by:

$$\mathbf{D}_t = g(\mathbf{F}_t, \mathbf{v}_t), \quad \mathbf{v}_t \sim \mathcal{N}(\mathbf{0}, \boldsymbol{\Sigma}_v). \quad (1)$$

In this very general framework, the functional form of the observation equation is unknown and potentially highly non-linear. To model the relationship between the observed variables and the latent factors I approximate function g via dimension reduction techniques. That is, we learn the latent factors and obtain its estimates $\hat{\mathbf{F}}_t$ via linearly and non-linearly compressing its dimension with methods discussed in Section 2.1.

A suitable econometric model which combines unobserved and observed variables in a vector autoregression is the factor-augmented vector autoregression model. Introduced by [Bernanke et al. \(2005\)](#), the FAVAR model is capable of achieving parsimony and at the same time including a broad range of information necessary to capture the dynamics in a large dataset. This is accomplished by assuming that the K -dimensional vector of endogenous variables \mathbf{y}_t is comprised of the set of latent factors \mathbf{F}_t and small number of R observed macroeconomic variables \mathbf{Z}_t (such as, e.g., the policy instrument), i.e., $\mathbf{y}_t = [\mathbf{F}_t', \mathbf{Z}_t']'$ (with $K = R + Q$) and follows a VAR model with p lags given by

$$\mathbf{y}_t = \mathbf{c} + \mathbf{A}_1 \mathbf{y}_{t-1} + \dots + \mathbf{A}_p \mathbf{y}_{t-p} + \boldsymbol{\epsilon}_t, \quad (2)$$

where \mathbf{c} denotes the K -dimensional vector of constants and the $K \times K$ matrices $\mathbf{A}_1, \dots, \mathbf{A}_p$ contain the reduced form coefficients for each lag and $\boldsymbol{\epsilon}_t$ is the normally distributed error term with zero mean and a $K \times K$ variance-covariance matrix $\boldsymbol{\Sigma}_\epsilon$.

I apply the two-step approach as in, e.g., [Bernanke et al. \(2005\)](#), [Boivin et al. \(2009\)](#) and [Korobilis \(2013\)](#) and start by estimating the latent factors in Eq. 1. Section 2.1 provides deeper insights into the first step of the procedure. Next, the dynamics of the factors are estimated in a Bayesian VAR model. I apply the standard Minnesota prior on the VAR coefficients to shrink unimportant coefficients towards zero ([Doan et al., 1984](#); [Sims and Zha, 1998](#); [Giannone et al., 2015](#)). Details on the prior specifications can be found in Appendix B. Since a structural analysis of the system (e.g., impulse response analysis) needs some kind of effect size measures, I use a linear approximation which captures the functional relationship between the variables similar to regression coefficients. This way I make sure that the process is computationally tractable even if a closed-form inverse is not available, what is the case in many highly non-linear models. A detailed discussion is provided in Section 2.2.

2.1 Dimension reduction techniques

For extracting estimates of the latent factors $\hat{\mathbf{F}}_t$ I implement three different dimension reduction techniques. First, the construction of principal components (PCs) allows to implement the standard approach, referred to as the linear FAVAR. Second, I use locally linear embedding (LLE) from the manifold learning literature, labeled *Locally Embedded FAVAR*. Third, I construct the latent factors by applying an autoencoder and refer to it as the *Deep Dynamic FAVAR*. With this modeling choices the aim is to elaborate on the impact of different degrees of non-linearities. Manifold learning techniques can be seen as a generalization of PCA, which are able to preserve

the global structure of the data even if it does not lie in a linear subspace (Roweis and Saul, 2000; Bengio et al., 2013). The autoencoder, on the other hand, is based on neural networks and, as such, is able to learn any functional form under relatively few assumptions (Hornik et al., 1989; Bank et al., 2023). It is the most flexible approach I test in this setup in order to learn the structure of the data. As emphasized in Section 2, the general FAVAR model is not limited to those dimension reduction techniques but is capable of incorporating various functional forms to obtain the latent factors.

Linear FAVAR. The most popular and commonly used dimension reduction technique to obtain latent factors is principal component analysis (PCA). The principal components of \mathbf{D} are obtained by performing a truncated singular value decomposition (SVD) of the sample covariance matrix of \mathbf{D} . The resulting factor matrix $\hat{\mathbf{F}}$ is of dimension $T \times Q$ and, for an appropriate Q , summarizes the main information in the data (Stock and Watson, 2002). Formally, the latent factors are defined $\hat{\mathbf{F}}$ as

$$\hat{\mathbf{F}} = \mathbf{D}\Lambda(\mathbf{D}'\mathbf{D}), \quad (3)$$

with Λ being the truncated eigenvector matrix of $\mathbf{D}'\mathbf{D}$ with dimension $N \times Q$.

Locally Embedded FAVAR. Originating from the field of image recognition, methods from the manifold learning literature are increasingly used in various research areas that deal with high-dimensional datasets. One of these non-linear methods for dimensionality reduction is locally linear embedding (LLE) introduced by Roweis and Saul (2000). The algorithm aims to infer a lower-dimensional representation of the dataset while trying to preserve its geometric features.

This is done by finding the k -nearest neighbors of each column $\mathbf{d}_{\bullet i}$ ($i = 1, \dots, N$) of \mathbf{D} and approximating the vector by weighted linear combinations of its k -nearest neighbors. We determine the k -nearest neighbors in terms of the Euclidean distance and select the optimal number of k by applying the algorithm of Kayo (2006). The algorithm preselects a set of potential candidates for k and then runs through the steps in the LLE algorithm to find its optimal value. For the approximation of the data vectors, the weight matrix $\mathbf{\Omega}$ for the linear combinations of the k -nearest neighbors is obtained by minimizing the following cost function:

$$C(\mathbf{\Omega}) = \sum_i (\mathbf{d}_{\bullet i} - \sum_j \omega_{ij} \mathbf{d}_{\bullet j})^2, \quad (4)$$

where ω_{ij} denotes the (i, j) th element of $\mathbf{\Omega}$. This minimization problem is subject to two constraints. First, matrix $\mathbf{\Omega}$ must be row-stochastic, i.e. each row of the matrix sums to one. Second, the reconstruction of each $\mathbf{d}_{\bullet i}$ is only considering its neighbors, implying non-zero weights only if $\mathbf{d}_{\bullet j}$ is a neighbor of $\mathbf{d}_{\bullet i}$.

Given the optimal weights, the algorithm requires the minimization of the cost for $\hat{\mathbf{F}}$ being

the new data points given by

$$\Phi(\hat{\mathbf{F}}) = \sum_i |\mathbf{f}_{\bullet i} - \sum_j \Omega_{ij} \mathbf{f}_{\bullet j}|^2, \quad (5)$$

with $\mathbf{f}_{\bullet i}$ denoting the i th column of $\hat{\mathbf{F}}$. To obtain a well-behaved problem $\mathbf{f}_{\bullet i}$ is constrained to have zero mean and unit variance. The factors are then extracted by solving

$$\mathbf{M} = (\mathbf{I}_t + \mathbf{\Omega})'(\mathbf{I}_t + \mathbf{\Omega}) \quad (6)$$

and finding the $Q + 1$ eigenvectors of \mathbf{M} corresponding to the $Q + 1$ smallest eigenvalues. Discarding the bottom eigenvector gives the Q factors, which represented the dataset in a low-dimensional and neighborhood-preserving manner.

Deep Dynamic FAVAR. For the Deep Dynamic FAVAR model, the latent factors $\hat{\mathbf{F}}$ are obtained by implementing an autoencoder and making use of the non-linear, lower-dimensional representation of the dataset. Belonging to the family of deep learning algorithms, autoencoders non-linearly convert a high-dimensional input to a transformed representation by first encoding the input to a lower-dimensional internal representation (the latent factors) and then decoding those latent factors back to the original dimension.

Autoencoders enjoy increasing attention in econometric analysis. First applications in economic forecasting and economic modeling can be found in, e.g., Heaton et al. (2017); Farrell et al. (2018); Feng et al. (2018a); Kelly et al. (2018); Cabanilla and Go (2019); Dixon and Polson (2019); Andreini et al. (2020); Hauzenberger et al. (2020). The proposed Deep Dynamic FAVAR approach is closely related to the recent literature dealing with factor models in combination with autoencoders or deep neural networks (Cabanilla and Go, 2019; Dixon and Polson, 2019; Andreini et al., 2020). Extending these concepts for structural analysis, I incorporate the highly non-linear factors to a VAR setting.

In contrast to the dimension reduction techniques discussed so far, deep learning algorithms generate the latent factors by learning the functional form of the observation equation in Eq. 1. This is done by introducing a set of parameters, which are optimized to find a good representation of the dataset (Goodfellow et al., 2016). In particular, the algorithm involves applying a number of $l \in \{1, \dots, L\}$ non-linear transformations, i.e., activation functions, to \mathbf{D} . I repeat this process in L hidden layers. The number of neurons which are input to the transformation process in each hidden layer is denoted by m_l . That is, in each layer a univariate activation function denoted by h_1, \dots, h_L is applied to the neurons of the previous layer collected in matrix $\hat{\mathbf{D}}^{(l)}$. Note that for the first layer this corresponds to the original dataset ($\hat{\mathbf{D}}^{(1)} = \mathbf{D}$). Formally, this boils down to

$$h_l^{W^{(l)}, b_l} = h_l \left(\sum_{i=1}^{m_l} \mathbf{W}_{\bullet i}^{(l)} \hat{\mathbf{d}}_{\bullet i}^{(l)} + b_l \right), \quad 1 \leq l \leq L, \quad (7)$$

with $\hat{\mathbf{d}}^{(l)}$ denoting the i th column of matrix $\hat{\mathbf{D}}^{(l)}$. The parameters of the activation function to be determined are $\mathbf{W}^{(l)}$, which represents a weighting matrix and b_l , which denotes a bias

term associated with layer l . $\mathbf{W}_{\bullet i}^{(l)}$ corresponds to the i th column of the weighting matrix. By minimizing a loss function of choice, the optimal values for the weight matrix and the bias term for each layer are determined. The estimation of these parameters is crucial. Provided that the algorithm adopted learns the correct parameters, a feed-forward network such as the autoencoder can basically approximate any functional form. This implies that, given the optimal parameters, the autoencoder can model the relationships in an underlying dataset regardless of their complexity and non-linearity (Hornik et al., 1989; Hornik, 1991; Goodfellow et al., 2016).

Finally, the deep dynamic factors $\hat{\mathbf{F}}$ are extracted after applying L layers to the dataset:

$$\hat{\mathbf{F}} = (h_1^{W^{(1)}, b_1} \circ \dots \circ h_L^{W^{(L)}, b_L})(\mathbf{D}). \quad (8)$$

Table 1: Summary of the model features for the Deep Dynamic FAVAR

	Hyperparameter	Sets in the cross validation	Final choice
Model structure	number of latent factors	{2,3,4,5,6}	5
	number of hidden layers	{1,2,3,4,5}	3
	number of neurons for each layer	evenly downsizing the original dimension	{126, 86, 46}
	penalisation	none	none
	dropout layers and rates	none	none
	batch norm layers	none	none
	activation function	tanh and ReLU	ReLU
Optimization	size of mini batches	24	24
	number of epochs	100	100
	optimization algorithm	Adam with default parameters	Adam
	loss function	mean squared error	mean squared error

Note: The table gives details on the sets of parameters used in the cross validation and on the final choice of parameters used in the algorithm.

The deep dynamic FAVAR depends on a large set of hyperparameters. In the empirical application, I choose the hyperparameters according to the results of a cross validation exercise. The final model is comprised of five latent factors, three hidden layers with 126 neurons in the first hidden layer, 86 neurons in the second and 46 neurons in the third hidden layer. The activation function suggested by the cross validation exercise is ReLU. Glorot et al. (2011), for example, show that ReLU is often preferred to other activation functions because rectifying neurons are capable of creating a sparse representation of the dataset. As the most common choices for the loss function and optimization algorithm, I use a mean squared error loss function and adaptive moment estimation (Adam). For the optimization of the algorithm, I use 24 minibatches corresponding to the average duration of a business cycle in the US, i.e., six years.¹ The optimization algorithm is repeated in 100 epochs. Table 1 provides an overview of all choices on the deep learning algorithm implemented for the empirical application.

¹The National Bureau of Economic Research publishes data on the duration of US business cycle expansions and contractions what allows for a determination of the average duration of a business cycle in the US. Details on the data can be found in Appendix C.

2.2 Linear approximation for measuring effect sizes of highly non-linear models

I wish to study how the economy reacts to structural shocks. This is achieved by comparing impulse response functions. For the FAVAR approach, this analysis requires a mapping between the latent factors \mathbf{F}_t and the underlying macroeconomic and financial variables in \mathbf{D}_t . Especially, when dealing with non-linear latent factors there is the need for an effect size measure similar to a regression coefficient that enables the estimation of the relationship between the factors and the dataset even in highly non-linear models. As many of these models are not computationally tractable, there is the need for approximations in order to measure the effects of the latent factors on the observed variables. I suggest using a linear approximation, which originates from the machine learning literature and the attempt of estimating effect sizes in black-box models (Crawford et al., 2018, 2019). Huber et al. (2020), for example, use such approximations to cast highly non-linear models in a Gaussian state space form.

In particular, I apply the Moore-Penrose pseudoinverse, which allows for a linkage between the non-linear factors and the economic and financial variables in the dataset even if the inverse of the unobserved factor matrix \mathbf{F} does not exist (Theodoridis, 2015). I define \mathbf{F} as the full data matrix of the unobserved factors, i.e, $\mathbf{F} = (\mathbf{F}_1, \dots, \mathbf{F}_T)'$ and \mathbf{F}^+ as the Moore-Penrose pseudoinverse of \mathbf{F} . To find a set of linearized coefficients $\hat{\boldsymbol{\theta}}$ I solve

$$\hat{\boldsymbol{\theta}} = \text{Proj}(\mathbf{F}, \mathbf{D}) = \mathbf{F}^+ \mathbf{D},$$

with $\mathbf{D} = (\mathbf{D}_1, \dots, \mathbf{D}_T)'$. Note that if \mathbf{F} has full rank $\hat{\boldsymbol{\theta}}$ produces the least squares estimate of $\boldsymbol{\theta}$. If \mathbf{F} has less than full rank, the application of the Moore-Penrose pseudoinverse makes sure that the correct fitted values for \mathbf{D} can be found.

3 Identification strategy

When it comes to analyzing the effect of economic shocks on a set of macroeconomic variables the reduced form residuals in the model described above are not the ones of main interest. Instead we would like to recover the structural shocks of the VAR model. These, however, are only identified with further restrictions. Proposals in the literature involve restrictions on short- or long-run responses of variables (see, e.g., King et al., 1991; Bernanke et al., 2005; Christiano et al., 2005; Stock and Watson, 2005; Pagan and Pesaran, 2008), or on the sign of impulse responses (see, e.g., Uhlig, 2005; Baumeister and Hamilton, 2015; Ahmadi and Uhlig, 2015; Antolín-Díaz and Rubio-Ramírez, 2018). Other studies suggest using dynamics in volatilities of the residuals (see, e.g., Rigobon, 2003; Lanne and Lütkepohl, 2008, 2010; Lütkepohl and Woźniak, 2020) or introducing proxy variables (see, e.g., Bloom, 2009; Mertens and Ravn, 2013; Carriero et al., 2015; Gertler and Karadi, 2015; Angelini and Fanelli, 2019). In the empirical section of the paper, I implement two applications with different identification strategies. While the first one relies on short-run restrictions justified by plausible economic reasoning, the second application involves estimating a proxy variable for uncertainty.

The monetary policy shock is modelled with identification by short-run restrictions. This

strategy is based on economic reasoning and restricts contemporaneous effects of certain variables to be zero (see, e.g., Bernanke et al., 2005; Christiano et al., 2005; Stock and Watson, 2005; Boivin et al., 2009). The implementation of this idea involves orthogonalizing the reduced form errors, i.e., making the errors mutually uncorrelated. This is obtained by Cholesky decomposition and results in a recursive structural model, which requires an ordering based on economic justifications (Kilian and Lütkepohl, 2017). I divide the dataset into fast- and slow-moving variables based on theoretical considerations and economic intuition as suggested by Bernanke et al. (2005). Fast-moving variables include financial variables, prices and monetary aggregates and are assumed to respond immediately to unanticipated shocks. Slow-moving variables, such as wages or consumption, do not show contemporaneous effects after a monetary policy shock by assumption. A detailed description of the dataset including the classification of the variables are presented in Appendix C.

The second empirical application involves identifying an uncertainty shock, which is achieved by estimating the structural vector autoregression with an external instrument (or Proxy-SVAR). I follow Jurado et al. (2015) and construct an uncertainty index, which functions as the instrument (or proxy) variable. I define the measure of uncertainty as the volatility of expected forecast errors. In particular, I construct an uncertainty estimate of each variable in the dataset by applying the stochastic volatility approach of Kastner and Frühwirth-Schnatter (2014) and extract one common factor by using the first principal component of the covariance matrix of all uncertainty estimates. For further details on the approach I refer to Jurado et al. (2015). Having obtained the proxy for uncertainty, I include it in the set of endogenous variables and order it first in the VAR (see, e.g., Bloom, 2009; Koop and Korobilis, 2014; Carriero et al., 2015; Jurado et al., 2015; Baker et al., 2016; Carriero et al., 2018, 2021).

4 Simulation study

In this section I apply the proposed FAVAR approaches to synthetic data and investigate the properties of the non-linear models in more detail. I do so by conducting a fully-fledged out-of-sample forecasting exercise. To mimic the complex dynamics observed in macroeconomic and financial variables during severe crises such as the COVID-19 pandemic, I introduce nonlinearities in the data generating process (DGP). This is achieved by modeling a non-linear VAR structure, which generates outliers in the data. Moreover, I assume that the covariation in the synthetic series can be captured by a few latent factors and that the relationship between the main dataset and the latent factors is non-linear.

In particular, the relationship between the main dataset \mathbf{D}_t and the latent factors \mathbf{y}_t is given by

$$\mathbf{D}_t = \boldsymbol{\lambda}(\mathbf{y}_{t-1}\mathbf{y}_{2,t-2}) + \mathbf{v}_t, \quad \mathbf{v}_t \sim N(0, \boldsymbol{\Sigma}_v).$$

I assume that \mathbf{y}_t is a 3-dimensional vector of latent factors. \mathbf{D}_t denotes the observed dataset including 20 variables which are observed for 350 periods ($T = 350$). $\boldsymbol{\lambda}$ denotes the matrix capturing the factor loadings which is of dimension 20×3 and sampled from a $\mathcal{N}(0, 0.1^2)$ distribution. The variance-covariance matrix $\boldsymbol{\Sigma}_v$ is the identity matrix with dimension 20×20 .

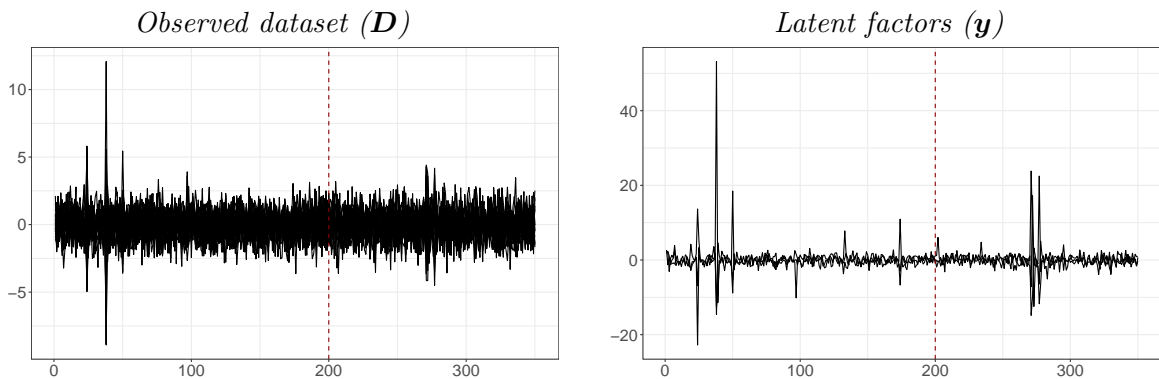
For the non-linear VAR, I let \mathbf{A}_1 and \mathbf{A}_2 denote a 3×3 coefficient matrix with off-diagonal elements sampled from a normal distribution of the form $\mathcal{N}(0, 0.1^2)$. Centering all coefficients on 0 ensures stationarity of the data. Moreover, I define \mathbf{C} as a lower triangular matrix with off-diagonal elements drawn from a normal distribution given by $\mathcal{N}(0, 0.1^2)$ and diagonal elements set to 1. The latent factors are then modelled as:

$$\mathbf{y}_t = \mathbf{A}_1(\mathbf{y}_{t-1} \mathbf{y}_{2,t-2}^{-1}) + \mathbf{A}_2(\mathbf{y}_{t-1} \mathbf{y}_{3,t-1}) + \mathbf{C} \mathbf{u}_t, \quad \mathbf{u}_t \sim N(\mathbf{0}, \mathbf{I}).$$

I take 20 random samples from the data generating process (DGP) and conduct an out-of-sample forecasting exercise with the three competing FAVAR approaches discussed in Section 2. The hold-out is comprised of the last 200 periods. I compute the predictive densities on an expanding window basis, i.e., I forecast the first period in the hold-out only with the data up to this point and repeatedly add the subsequent observation until I end up at the end of the sample.

Figure 1 presents one randomly selected realization from the DGP described above with the left panel plotting all variables in the dataset and the right panel plotting the latent factors. Mimicking ups and downs of the business cycle as well as severe crises such as the COVID-19 pandemic, the DGP includes substantial movements and severe outliers next to more quiet periods over the sample.

Figure 1: Simulated dataset.



Note: The graph shows all observed variables (left panel) and the latent factors (right panel) from a randomly selected sample of the non-linear DGP.

To evaluate the performance of the different models, Table 2 reports root mean squared errors (RMSEs) for point forecasts and continuous ranked probability scores (CRPS, [Gneiting and Raftery, 2007](#)) for density forecasts. All values are relative to the linear model. To gain deeper insights on the benefits of the non-linear approaches and when they are most pronounced I separately evaluate the forecasting performance during highly volatile and tranquil periods of the DGP. This is accomplished by labeling periods in which the latent factors exceed the interquartile range by a factor of seven as “Crisis Times”. Moreover, I allocate variables to different groups depending on how severely they are affected by highly volatile periods. This allocation is carried out by clustering variables whose values exceed the interquartile range by certain levels. Variables classified as “heavily affected” are those exhibiting outliers that exceed the interquartile range by a factor of seven. “Affected” defines variables with outliers

Table 2: Relative point and density forecasting performance for simulated data

Model	Variables	Crisis Times		Tranquil Times	
		RMSE	CRPS	RMSE	CRPS
Deep Dynamic FAVAR	Overall	0.92	0.92	1.01	1.01
	Heavily affected	0.87	0.86	1.03	1.01
	Affected	0.91	0.91	1.00	1.00
	Not affected	0.87	0.83	0.98	0.99
Locally Embedded FAVAR	Overall	0.99	0.99	1.00	1.00
	Heavily affected	0.98	0.98	1.00	1.01
	Affected	0.99	0.99	1.00	1.00
	Not affected	0.94	0.90	1.00	1.00

Note: The table shows point forecasting performance in terms of root mean squared errors (RMSE) as well as density forecasting performance in terms of continuous ranked probability scores (CRPS). All metrics are relative to the linear FAVAR. Values below one (bold numbers) show that the non-linear model outperforms the linear one. Variables are separated depending on how strongly they are affected by crises. “Heavily affected” defines variables exhibiting outliers that exceed the interquartile range by a factor of seven. “Affected” variables are those with outliers exceeding two times the interquartile range. Variables without any outliers are classified as “not affected”.

exceeding two times the interquartile range. All other variables, where no outliers are detected, are included in “not affected”.

Overall, I find that major gains from using non-linear models are obtained during highly volatile times. The Deep Dynamic FAVAR, being the most flexible model, outperforms the other two approaches by significant margins. This holds for point as well as for density forecasting performance. Improvements of the Locally Embedded FAVAR against the linear approach are rather small when averaging across all variables.

Zooming into the different groups of variables reveals that the Deep Dynamic FAVAR gives the highest forecasting accuracy for heavily affected variables, closely followed by variables being not affected. Those gains are high in terms of RMSEs and even higher when considering CRPS. This implies that the deep learning model flexibly adapts to times of high uncertainty and is able to spread its strengths to many variables in the system. This can also be seen in Table 3 in Appendix A, which shows the forecasting performance of each variable. Evidently, the improvement of the Deep Dynamic FAVAR upon the linear model is not restricted to a few specific variables but can be found across most of them. The Locally Embedded FAVAR shows some gains for heavily affected models which are, however, rather small. Highest gains can be found for variables without outliers. From this I conclude that this model is also able to handle certain degrees of non-linearities but is not flexible enough to accurately model the highly affected and affected variables.

For tranquil times all models yield a very similar performance. This suggests that highly non-linear techniques benefit the most against linear models when data is characterized by high volatility and complex relationships between variables. Nonetheless, I do not see any adverse effects of the high flexibility of the deep learning model or the locally linear embedding approach when variables show unobtrusive behavior.

5 Empirical application

In this section, I first introduce the dataset for the empirical application and provide an in-depth analysis of the latent factors. The discussion of the latent factors obtained from the different approaches in a profound manner helps to achieve a better understanding of the role of potential non-linearities and to give basic economic interpretation. I proceed with presenting the results of the impulse response analysis of a monetary policy shock as well as an uncertainty shock before and during the COVID-19 pandemic. I compare the responses of selected macroeconomic and financial quantities between linear and non-linear FAVAR models to investigate whether controlling for non-linearities alter the results.

5.1 Data

I use 166 quarterly variables from the US database discussed in [McCracken and Ng \(2020\)](#). The data runs from 1965Q1 to 2020Q4. I assess and compare the properties of the different FAVAR approaches for the period before the COVID-19 outbreak (i.e., 1965Q1 - 2019Q4) and for the period including the COVID-19 pandemic (i.e., 1965Q1 - 2020Q4). For the data transformation, I choose a mixed approach where most variables are included with year-on-year growth rates and some enter the analysis in levels. A detailed description of the data transformation can be found in [Appendix C](#). Each time series is standardized to get series with zero mean and unit sample variance.

Similar to [Bernanke et al. \(2005\)](#), the observed variables included in the VAR are industrial production, the unemployment rate, inflation and the policy instrument. Since the sample includes the prolonged period at the zero lower bound, I choose the shadow federal funds rate as the policy measure (see, e.g., [Damjanovic and Masten, 2016](#); [Potjagailo, 2017](#); [Lombardi and Zhu, 2018](#)). In particular, I use the shadow rate suggested by [Wu and Xia \(2016\)](#), who show that their measure allows to study the reaction of macroeconomic variables to monetary policy even when hitting the zero lower bound.

The latent factors are obtained by reducing the dimension of all other variables ($N = 162$). The number of factors to be included in the model is chosen according to the cross validation exercise for the autoencoder which suggests a number of five factors (i.e., $Q = 5$). Moreover, a closer examination of the principal components obtained from the linear approach shows that the first five factors explain close to 70 % of the variation in the input dataset what seems to be reasonably high. The lag order is set equal to four ($p = 4$).

5.2 Structure of the latent factors

In this section, I discuss the properties of the factors obtained from the different dimension reduction techniques presented in [Section 2.1](#). Since the FAVAR model is based on the assumption that the main dynamics of the economy can be captured in a lower dimensional representation, the latent factors play a key role. Depending on the method used to extract them, they may significantly differ in processing the signals they receive from variables in the underlying dataset. I focus on two aspects: First, I compare the shape of each factor obtained from the three dimension reduction techniques. This way, I can shed light on the effect of potential non-linearities.

Second, I identify the 15 most important variables characterizing the factors, which allows to give them an economic meaning. For each factor I provide a figure comprised of four plots including the respective time series in the upper panel and the variable importance measures in the lower panel. Given that the dataset is extensive and includes a large number of variables, I also summarize variable importance for each factor across groups (as specified in McCracken and Ng, 2020) to gain a digestible overview.

Figure 2: Importance of different groups to latent factors.



Note: The graph shows variable importance according to factor loadings for the linear FAVAR and the Locally Embedded FAVAR and Shapley values for the Deep Dynamic FAVAR. Values are averaged across variables belonging to a specific group defined as in McCracken and Ng (2020). *HH* stands for households and *NIPA* is the National Income and Product Accounts.

Since I use linear and non-linear techniques to reduce the dimension of the dataset, the variable importance measure needs to be adapted accordingly. The variable importance for the linear FAVAR as well as the Locally Embedded FAVAR is given by absolute factor loadings. Due to its non-linear structure the Locally Embedded FAVAR needs minor modifications, which I borrow from the Neighborhood Preserving Embedding algorithm proposed by He et al. (2005). The main modification boils down to a linear approximation of the last step (i.e., Eq. 6) in the LLE algorithm. The resulting standard eigenvalue problem allows to interpret the factor loadings in a similar manner to those of PCA. For the Deep Dynamic FAVAR I compute Shapley values for each factor to get the contributions of individual variables (Shapley, 1953; Lundberg and Lee, 2017). Details for both measures are given in Appendix B.4. To achieve maximal comparability, I map factors according to their highest absolute correlation with each factor of the linear FAVAR. That is, I identify the factor of the Locally Embedded FAVAR as well as the Deep Dynamic FAVAR showing the highest absolute correlation with the first factor of the linear FAVAR and order it first. I repeat this exercise for all factors.

Variable importance by group. I start our discussion with the importance of variables summarized by groups (i.e., averaging importance measures across variables for each group and factor). Figure 2 presents the groups according to their importance for the factors of each FAVAR model for 2019Q4 (left panels) and 2020Q4 (right panels). Darker colors indicate higher weights across the variables forming a specific group.

In general, I see that the factors cover variables from all groups. Some factors can be assigned to a specific group, others are influenced by variables stemming from various groups. For the linear FAVAR estimated with data ending before the COVID-19 pandemic, I can identify a few main drivers for each factor. The first factor is driven by price data, the second one by real activity growth. Housing variables explain the third factor whereas the fourth and fifth factors are influenced by earnings and productivity. When including the year 2020 the ranking of the main groups per factor is less clear, except for the third factor which is still mainly driven by developments in the housing sector. For the first factor, for example, I get similar weights on real activity measures, such as employment and industrial production but also on interest rates and prices. The last factor is mainly driven by the households balance sheets and monetary variables.

For the non-linear cases the following picture arises. The Locally Embedded FAVAR puts high weight on interest rates and stock market variables for all factors. This holds for the periods ending before and after the COVID-19 crisis. The factors estimated within the Deep Dynamic FAVAR up to 2019Q4 show high weights on variables from earnings and productivity (Factor 1, 3 and 4) as well as exchange rates and order positions (Factor 1). Factor 2 is also influenced by order positions and inventories whereas the fifth factor is driven by balance sheet measures. When including 2020 I can identify Factor 1 being driven by inventories, orders and sales, Factor 2 and 3 representing the financial situation of households via balance sheet measures and Factor 4 being influenced by interest rates and stock market variables. Factor 5 is shaped by developments in earnings and productivity.

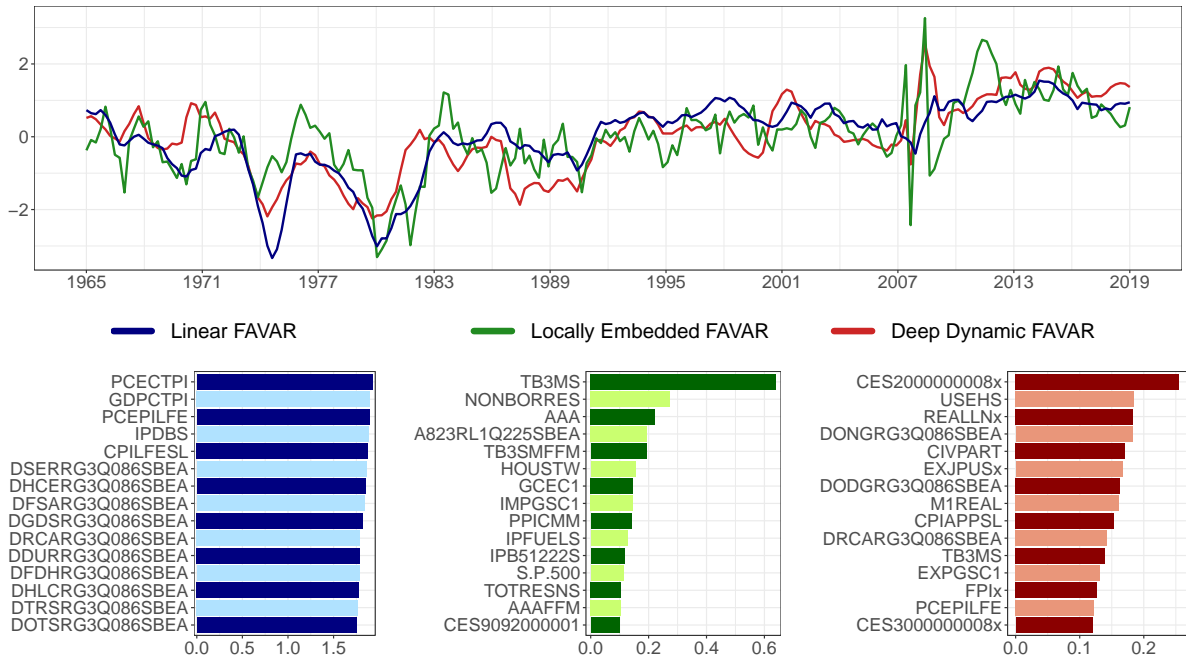
Variable importance and time series behavior. In the proposed general FAVAR setup, which includes linear and non-linear factor structures, it is not only important to identify the main drivers of the factors but also how the models extract the signals provided by variables with high weights. Hence, in the following I study closely the shape of the factors (time series plot in the upper panel) along with the main drivers (barplots in the lower panel). Figures for the sample including the COVID-19 period are relegated to Appendix A.

For the first factor up to 2019Q4, Figure 3 shows that all three approaches estimate strongest movements between the mid-1970s and the mid-1980s as well as during the Global Financial Crisis (GFC). This implies that the models successfully detect times of high uncertainty in the large-dimensional dataset. The linear factor attaches a lower degree of severity to the GFC than the other two models, which can be explained by the fact that it is mainly driven by inflation series. Top-15 variables for the first linear factor include consumer price indices as well as personal consumption expenditure price indices. On the contrary, the locally embedded factor shows high volatility during the GFC. This can be traced back to interest rates, money stock variables and bond yields, mainly influencing its shape. Given the composition and prevailing conditions of the GFC, monetary and financial variables were exposed to higher fluctuations than inflation. Among the most important variables shaping the deep dynamic factor I find real hourly earnings, employment and exchange rates. This explains the rather strong reaction to the GFC but to a lesser extent than the factor of the Locally Embedded FAVAR. When including the COVID-19 observations, there is little difference between the three methods (see Figure 10 in the appendix), especially, between the linear and the deep learning case. Both factors follow a very similar course over time and also show similarities with respect to variable importance. Main drivers are employment, business inventories and price series. The Locally Embedded FAVAR, on the other hand, is mainly driven by interest rates and variables from the national accounts.

Turning to the second factor, again, all factors differentiate between crisis and tranquil times, although attaching more weight on the dotcom bubble than in the previous case (see Figure 4). Moreover, the linear factor shows the largest outlier during the GFC, since it is now mainly driven by real activity variables (i.e., industrial production and employment), which were prone to high uncertainty during that time. The deep dynamic factor resembles the linear one with a lower reaction to the GFC. The most important variables include variables measuring the employment situation, producer price index for commodities and outstanding credits. The factor obtained from locally linear embedding shows the highest volatility and is again influenced by interest rates and nonborrowed reserves. Including data up to 2020Q4, as presented in Figure 11 in the appendix, changes the top variables for the linear factor to price and employment series and for the deep dynamic factor to variables measuring the employment situation, outstanding credit and money stocks. In the case of the locally embedded factor I identify stock market and housing variables in addition to the recurring importance of interest rates.

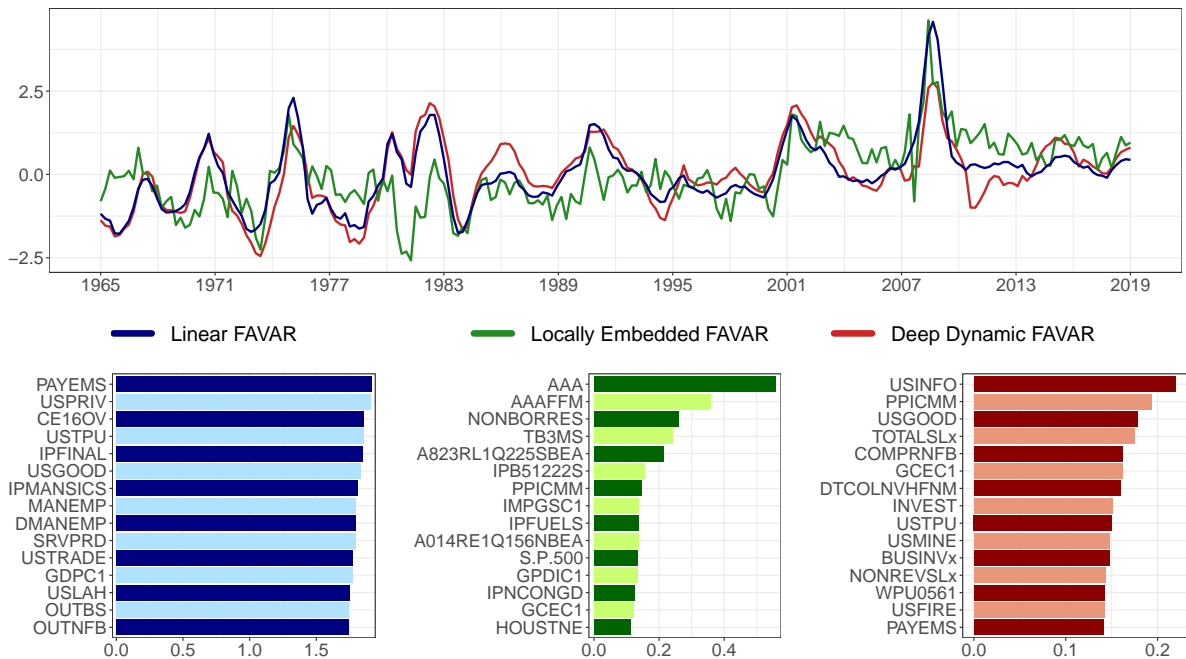
Inspecting the third factor (Figure 5 and Figure 12 in the appendix) reveals some interesting pattern of the linear model. It clearly peaks in advance to the non-linear methods for most crises, most importantly, for the Volcker period and the GFC. In the linear FAVAR model, Factor 3 is mainly driven by housing variables, which are often considered as leading indicators in the

Figure 3: First latent factor arising from linear and non-linear dimension reduction techniques and corresponding variable importance for 2019Q4.



Note: The upper panel depicts normalized factors of the three dimension reduction techniques (mapped according to the highest correlation) with mean zero and variance one obtained from the main dataset ($N = 162$) ranging from 1965Q1 to 2019Q4. The barplots show the 15 most important variables for each factor measured by the factor loadings for the linear FAVAR and the Locally Embedded FAVAR and Shapley values for the Deep Dynamic FAVAR. Mnemonics are those of McCracken and Ng (2020) and can be found in Appendix C.

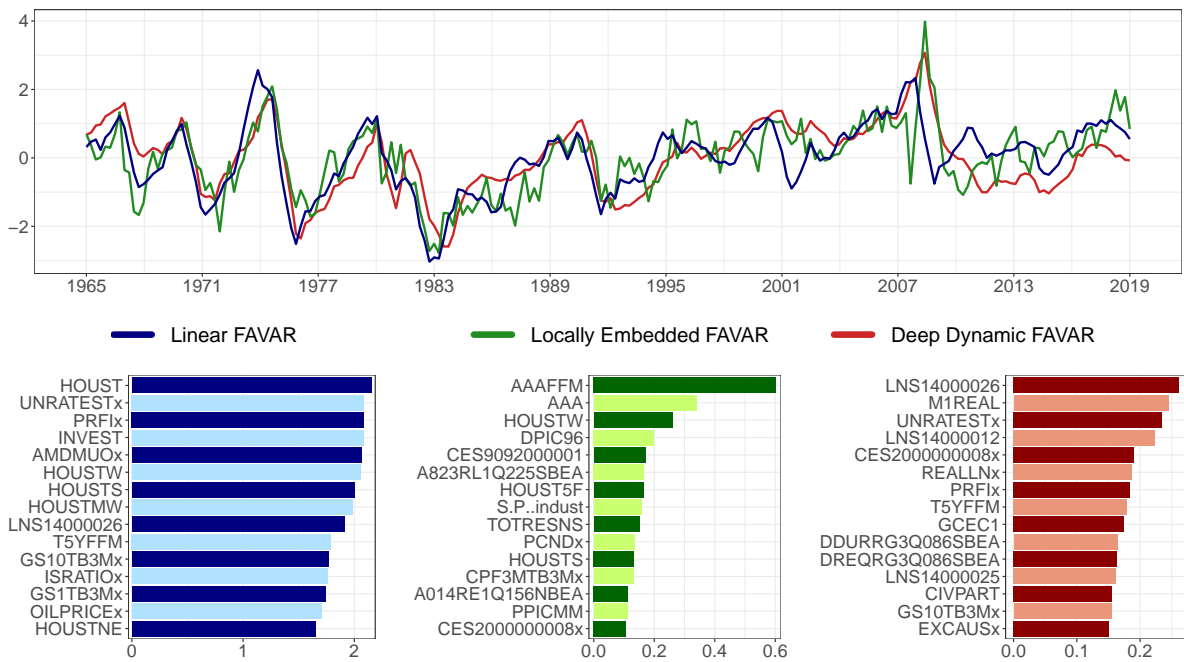
Figure 4: Second latent factor arising from linear and non-linear dimension reduction techniques and corresponding variable importance for 2019Q4.



Note: For more details I refer to Figure 3.

literature (see, e.g., Stock and Watson, 1989; Marcellino, 2006). The locally embedded factor up to 2019Q4 shows a similar behavior to its second counterpart with the most important variables being interest rates, housing starts and real disposable income. When including the COVID-19 observations I additionally observe importance of duration of unemployment. The deep dynamic factor is driven by employment variables and real money stocks for the case excluding COVID-19 periods. Considering the COVID-19 pandemic shifts highest importance to interest rates, real hourly earnings and dividend yield of the S&P 500 stock market index.

Figure 5: Third latent factor arising from linear and non-linear dimension reduction techniques and corresponding variable importance for 2019Q4.

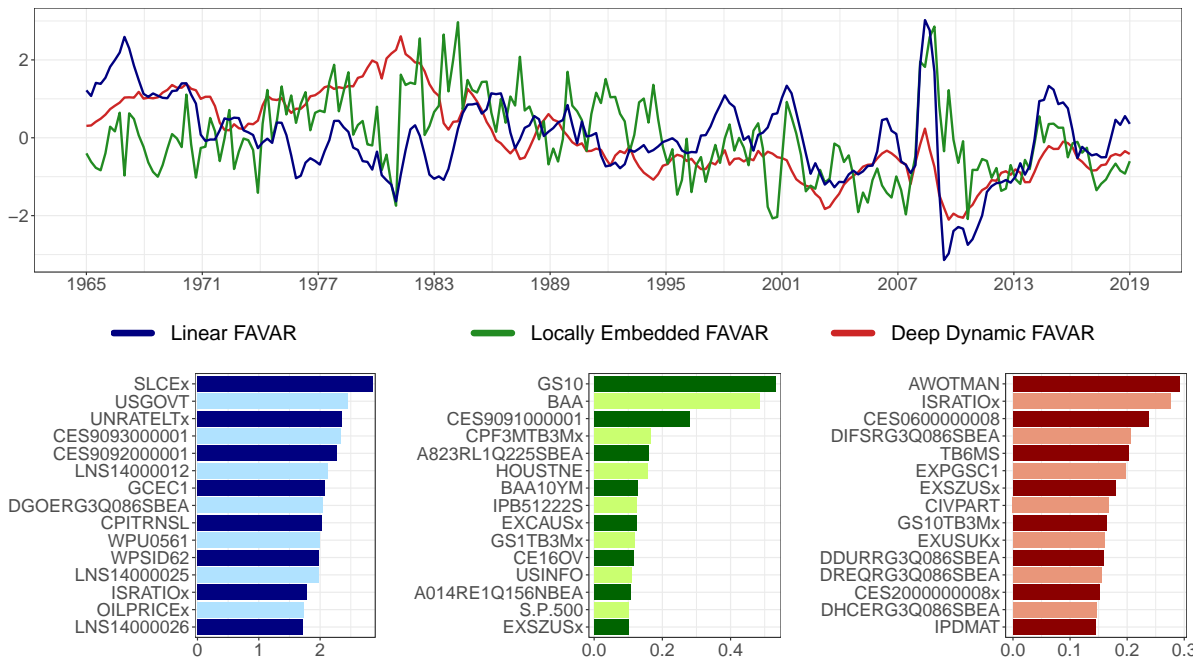


Note: For more details I refer to Figure 3.

Compared to Factors 1, 2 and 3, the correlation between Factors 4 obtained from the different dimension reduction techniques decreases significantly (see Figure 6 and Figure 13 in the appendix). The Deep Dynamic FAVAR yields a relatively smooth factor without major fluctuations or outliers. On the contrary, the locally embedded factor is highly volatile and, similar to the linear case, spikes during the GFC. This holds for both sample periods considered. The most important variables describing the linear factor for both samples include government consumption and employment/unemployment measures. As for most factors obtained from locally linear embedding, the locally embedded factor is driven by interest rates and among the first three variables I also find employment. For the Deep Dynamic FAVAR considering the sample up to 2019Q4 most important variables are overtime hours, business inventories and average hourly earnings whereas for up to 2020Q4 real hourly earnings and other statistics for employment as well as government expenditure influence the factor most.

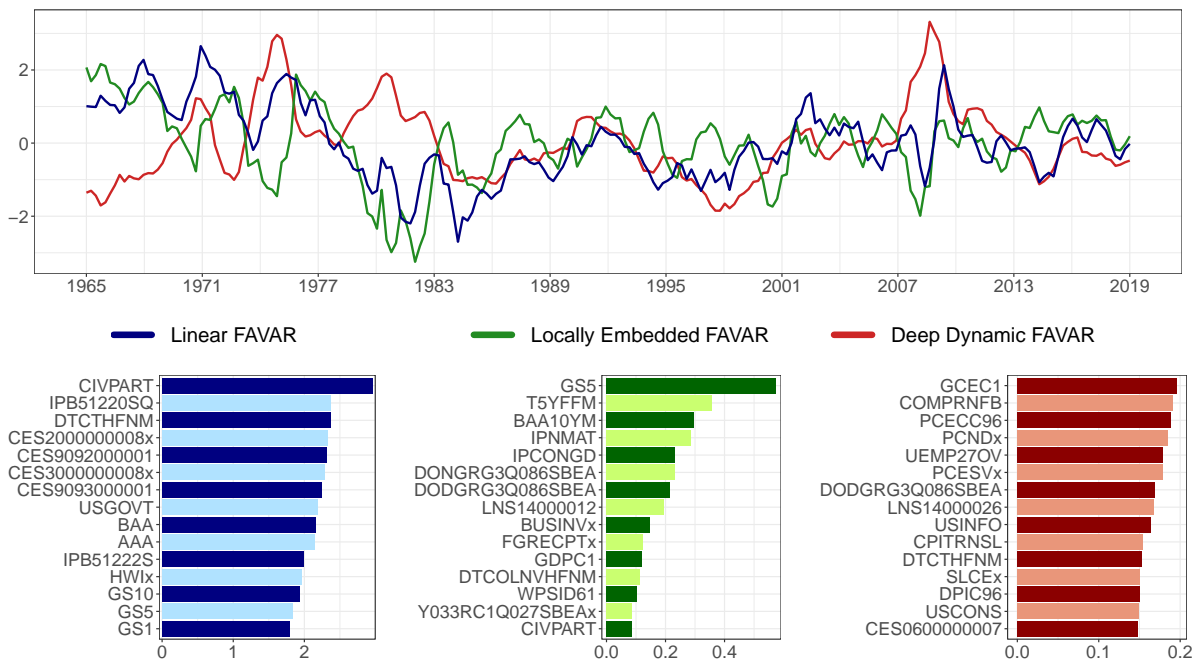
Similarly, Figure 7 shows that the last factor follows its own path for each model. While the linear and the locally embedded factor follow at least the same trend, the deep dynamic factor shows a different path. Its severest peaks can be found during the Volcker period as well as during the GFC when looking at the sample up to 2019Q4, which is still true when

Figure 6: Fourth latent factor arising from linear and non-linear dimension reduction techniques and corresponding variable importance for 2019Q4.



Note: For more details I refer to Figure 3.

Figure 7: Fifth latent factor arising from linear and non-linear dimension reduction techniques and corresponding variable importance for 2019Q4.



Note: For more details I refer to Figure 3.

including data up to 2020Q4 (see Figure 14 in the appendix). Top-3 drivers for up to 2019Q4 are government and personal consumption expenditures as well as real compensation per hour and for the full sample I get personal consumption expenditure price indices as well as the oil price. The linear FAVAR, on the other hand, reacts clearly to the COVID-19 pandemic. This

can be explained by the high influence of real activity measures such as industrial production and employment as well as loans. The factor obtained from the locally embedded FAVAR estimates the highest fluctuations during the GFC. Again, this behavior may be traced to the emphasis on interest rates and monetary variables.

Summing up this discussion, I find that the linear and the deep dynamic factors behave similarly for the first three factors but differ significantly for Factor 4 and 5. Both cover various sectors of the economy and often put high focus on real activity variables, prevailing financial conditions and price developments. The locally embedded factors are characterized by higher volatility and are concentrated on monetary variables.

5.3 Application 1 - Monetary policy shock

In the first empirical application, I simulate a 100 basis points (bps) expansionary monetary policy shock and compare the impulse responses generated by the different FAVAR approaches. I trace the responses of key macroeconomic and financial variables (i.e., output growth, unemployment rate, inflation, growth of housing starts, S&P 500 stock market index, short-term interest rate) over 16 periods (i.e., 4 years) after the shock hit the economy.

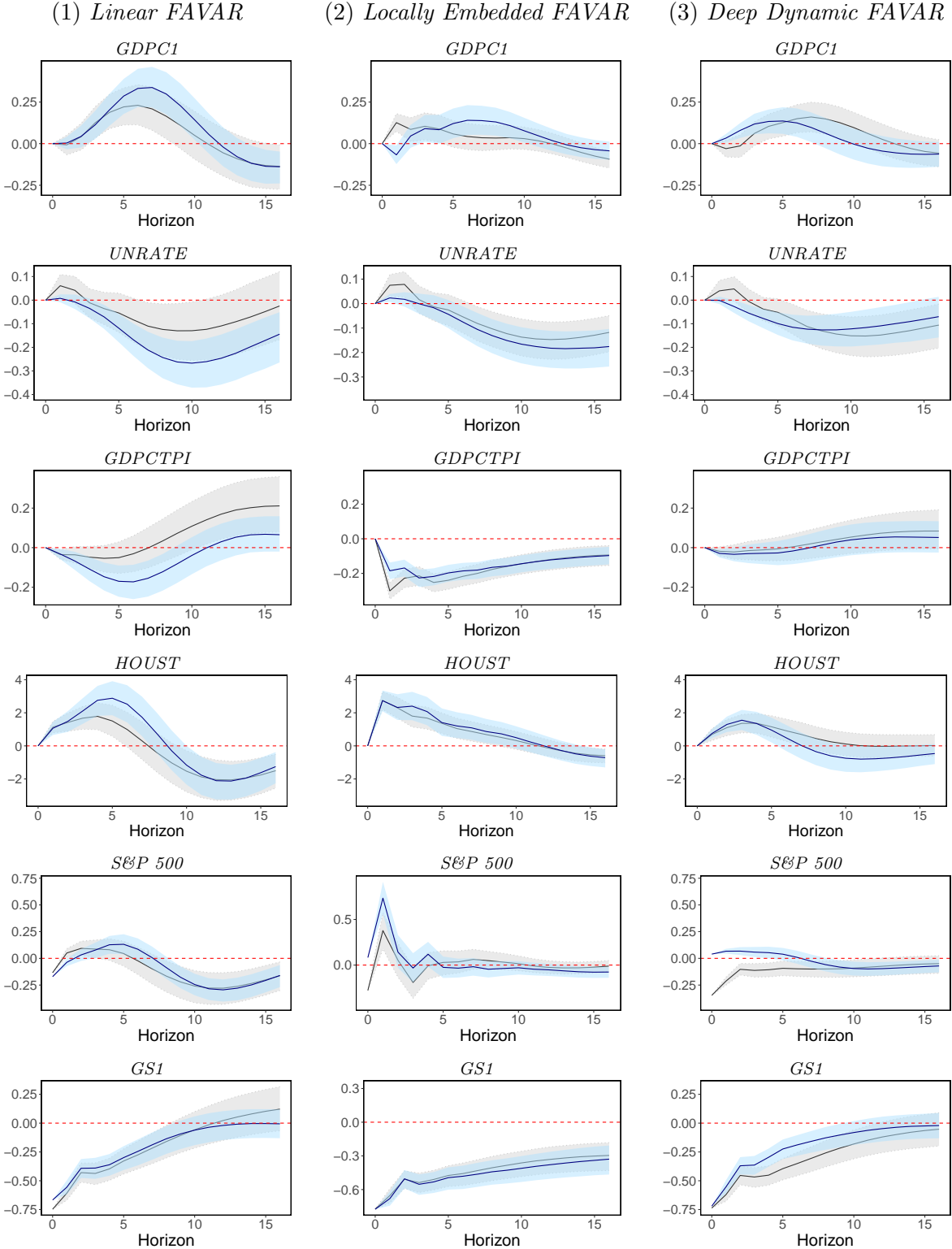
Figure 8 depicts the impulse responses of the different variables for an expansionary monetary policy shock based on data through 2019Q4, i.e. before the outbreak of COVID-19 and the same shock based on data through 2020Q4. I compare the responses of the linear FAVAR (panel 1), the Locally Embedded FAVAR (panel 2) and the Deep Dynamic FAVAR (panel 3). The blue solid line and the light blue shaded area depict the median and the 16th and 84th percentiles of the posterior distribution of the pre-pandemic responses, respectively. The black solid line and the grey shaded area correspond to the median response and the 16th and 84th posterior percentiles of the pandemic response.

Figure 8 reveals that the three different FAVAR approaches yield very similar responses of the variables of interest when modeling an expansionary monetary policy shock at the end of 2019. When including the pandemic observations I observe that the responses differ across the modeling techniques. The linear FAVAR yields responses that are surrounded by appreciable uncertainty bands. In contrast, the non-linear FAVAR models estimate similar reactions to the monetary policy shock in both scenarios (i.e., before and during the COVID-19 pandemic).

Comparing the responses of GDP growth (GDPC1) between the different FAVAR approaches suggests that all models yield similar results for the scenario excluding the COVID-19 pandemic. The peak is reached after six periods before approaching to zero and turning slightly negative. Considering the dataset ending in 2019, the linear FAVAR yields responses with the most pronounced impact estimate. When I include the pandemic observations, the linear FAVAR suggests a lower impact on GDP growth which is mainly insignificant. In contrast, the non-linear techniques yield significant and positive reactions similar to the case which excludes the pandemic. A similar pattern can be observed for the unemployment rate (UNRATE). Regardless of the included time periods, the non-linear approaches estimate a fall in the unemployment rate as a response to an expansionary monetary policy shock. The linear FAVAR, however, yields insignificant reactions when considering the dataset including the COVID-19 outliers.

For the inflation rate (GDPCTPI) differences between the responses of the models are more

Figure 8: Impulse responses of selected variables to a 100 bps expansionary monetary policy shock in 2019Q4 and 2020Q4 for the three different FAVAR approaches



Note: The blue solid lines refer to the median response and the light blue shaded area indicates the 16th and 84th percentiles of the posterior distribution for the data up to 2019Q4. The impulse responses including the COVID-19 observations are shown in grey. The median responses are presented in the black solid lines and the confidence bands in form of the grey shaded area. The red dashed line shows the zero line.

pronounced. The linear and Locally Embedded FAVAR estimated without pandemic observations yield negative reactions of inflation to the expansionary monetary policy shock during the first year after the shock hit the system. This stands in contrast with the results of the Deep Dynamic FAVAR which suggest a positive relationship between expansionary monetary policy shocks and inflation. Interestingly, when including pandemic observations the linear FAVAR model generates persistent and elevated reactions for inflation after six periods. The Locally Embedded FAVAR still yields a significantly negative reaction after the shock. The Deep Dynamic FAVAR, on the other hand, yields no significant reaction in this scenario.

Housing starts (HOUST) react positively to a cut in interest rates for all approaches when the pandemic observations are excluded. When taking the COVID-19 crisis into account, this pattern persists only for the non-linear models, i.e., Locally Embedded FAVAR and Deep Dynamic FAVAR. The linear FAVAR shows no significant reactions during the first year after the shock and even estimate negative responses for the second year after the shock.

For the S&P 500, I observe slightly negative reactions on impact for all FAVAR approaches when considering the data until the end of 2020. Excluding the observations of the pandemic leads to a reversal of this behavior for the Deep Dynamic FAVAR and the Locally Embedded FAVAR and suggests positive reactions of stock markets to an expansionary monetary policy shock. The Locally Embedded FAVAR is the only approach which estimates positive responses for two and three quarters after the shock in both scenarios.

The application of an expansionary monetary policy shock involves reducing the policy rate measured by the shadow rate by 100 bps on impact. As a consequence, the short-term interest rate (GS1) rate falls but slightly less than the 100 bps shock of the shadow rate. I observe this pattern for all models and both scenarios.

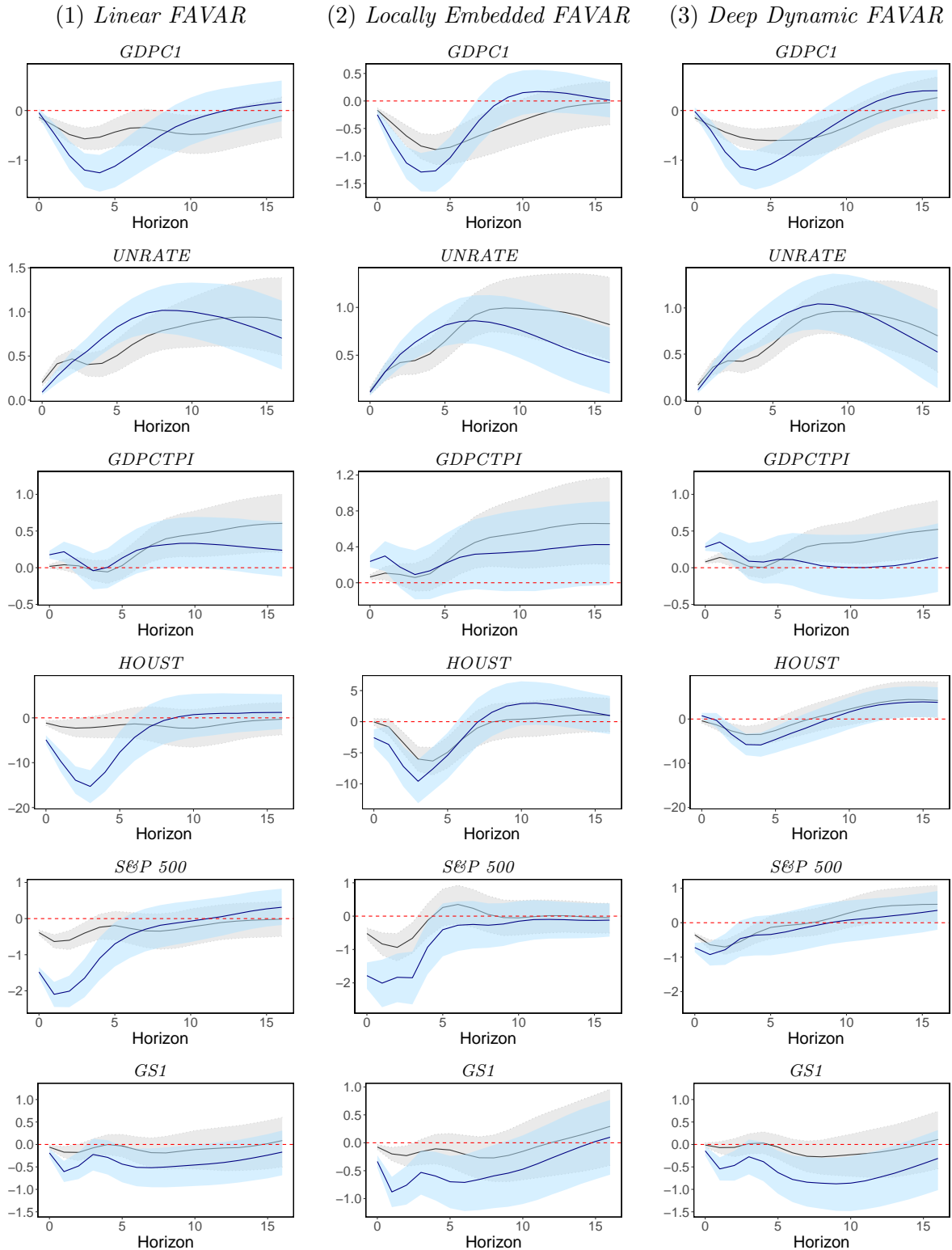
5.4 Application 2 - Uncertainty shock

In this section, I present the results of our second empirical application which involves simulating the effect of an uncertainty shock on key US macroeconomic and financial variables. As discussed in Section 3, I rely on the uncertainty index proposed by [Jurado et al. \(2015\)](#).² I compare the results of the three different FAVAR approaches introduced in Section 2 and show the impulse response functions for the same set of variables as in the previous section. Again, each panel of Figure 9 presents the impulse response function when using the dataset until the end of 2019 in blue and the extended version with the COVID-19 pandemic included in grey. The solid lines depict the median response while the blue and grey shaded areas correspond to the 16th and 84th percentiles of the posterior distribution.

As shown before, the impulse responses for the scenario excluding the pandemic observations are similar in all three FAVAR approaches with the main difference being that the linear FAVAR estimates the strongest effects for most variables. When extending the observation window to the end of 2020 I find that the effects are smaller and often insignificant if the linear FAVAR is adopted. The Deep Dynamic FAVAR, on the other hand, yields significant effects for all variables.

²Note that applying the National Financial Conditions Index (NFCI) as the uncertainty index yields very similar results.

Figure 9: Impulse responses of selected variables to a positive uncertainty shock (25 bps) in 2019Q4 and 2020Q4 for the three different FAVAR approaches



Note: The plot gives the impulse responses excluding the pandemic observations in blue, i.e., the blue solid lines refer to the median response and the light blue shaded area indicate the 16th and 84th percentiles of the posterior distribution. The impulse responses obtained when including the COVID-19 pandemic are shown in black. The median responses are presented in the black solid lines and the confidence bands in form of the grey shaded area. The red dashed line shows the zero line.

The first variable, GDP growth, falls in response to an uncertainty shock with a certain delay. The linear and the Deep Dynamic FAVAR estimate a quite strong reaction when the pandemic is excluded. When including the pandemic observations all approaches suggest a smaller reaction, with the Deep Dynamic FAVAR suggesting the strongest effect which is also quite long-lasting. The linear FAVAR as well as the Locally Embedded FAVAR yield less pronounced dynamics.

For the unemployment rate, all three FAVAR approaches produce very similar results. This is true for the scenario excluding as well as including the pandemic observations in the sample. The growth of unemployment rises in the periods following the uncertainty shock and peaks after seven to eight periods.

The inflation rate shows a positive reaction to the uncertainty shock on impact when considering the scenario before the COVID-19 pandemic. Estimating the models including the pandemic observations results in no significant reaction of inflation on impact but positive reactions after a year for the linear FAVAR and the Locally Embedded FAVAR. The Deep Dynamic FAVAR suggests a significantly positive reaction on impact and a positive reaction after about six periods.

For housing starts, I observe the largest differences between the models. The linear FAVAR suggest a strong negative reaction for data through 2019Q4. The peak is reached three periods after the shock hit the economy. However, when the sample is extended to the end of 2020 I see no significant reaction of the housing variable to the uncertainty shock. Similarly, the model based on the locally linear embedding algorithm yields a negative response on impact but no reaction for the scenario including the COVID-19 pandemic. For the Deep Dynamic FAVAR I observe a negative reaction for both scenarios, with and without COVID-19 observations, but the effect is slightly larger when excluding the pandemic.

Investigating the response of the S&P 500 stock market index reveals that on impact all models yield a significantly negative reaction. This effect is again strongest for the linear FAVAR when modelled without the COVID-19 periods. Including the pandemic observations also suggests a negative reaction on impact but to a far lesser extent. A similar pattern can be observed for the Locally Embedded FAVAR. The Deep Dynamic FAVAR suggests a similar negative response of the stock market index to the uncertainty shock in both scenarios.

For the short-term interest rate, I only observe a significant reaction to the uncertainty shock when leaving the pandemic observations aside. This pattern holds for all three modeling approaches.

6 Closing remarks

In this paper, I propose a set of high-dimensional non-linear factor models. By applying non-linear dimension reduction techniques to a high-dimensional dataset and assuming that the resulting latent factors evolve according to a vector autoregression, two novel approaches are developed. The first is the Locally Embedded FAVAR, which is based on the linear locally embedding algorithm and the second is the Deep Dynamic FAVAR, which employs a deep learning algorithm for constructing the lower-dimensional representation of a dataset.

When I apply the proposed techniques to synthetic data, allowing for an analysis of each model's behavior in a controlled environment, I find that the non-linear approaches yield com-

petitive forecasting performance across all hold-outs and outperform the linear model for highly volatile observations. Depending on the specific dimension reduction technique used, the factors differ in how they extract signals from macroeconomic and financial variables and cover various sectors of the economy. As I have shown in two different empirical applications, the proposed non-linear FAVAR approaches yield tight estimates and responses in line with economic theory. This is true for tranquil times as well as for times characterized by high uncertainty. Analyzing model performances in times of crises is of particular interest as the current COVID-19 pandemic has caused unprecedented fluctuations in various economic and financial variables.

The proposed model can be seen as a very general framework, which nests several functional forms to generate the series of latent factors. This is of interest for dealing with high-dimensional datasets as well as for analyzing dynamics in uncertain and highly volatile times.

References

- AHMADI, P. A., AND H. UHLIG (2015): “Sign restrictions in Bayesian FAVARs with an application to monetary policy shocks,” Discussion paper, National Bureau of Economic Research.
- ANDREINI, P., C. IZZO, AND G. RICCO (2020): “Deep dynamic factor models,” *arXiv preprint arXiv:2007.11887*.
- ANGELINI, G., AND L. FANELLI (2019): “Exogenous uncertainty and the identification of structural vector autoregressions with external instruments,” *Journal of Applied Econometrics*, 34(6), 951–971.
- ANTOLÍN-DÍAZ, J., AND J. F. RUBIO-RAMÍREZ (2018): “Narrative sign restrictions for SVARs,” *American Economic Review*, 108(10), 2802–29.
- BAKER, S. R., N. BLOOM, AND S. J. DAVIS (2016): “Measuring economic policy uncertainty,” *The Quarterly Journal of Economics*, 131(4), 1593–1636.
- BANK, D., N. KOENIGSTEIN, AND R. GIRYES (2023): “Autoencoders,” *Machine Learning for Data Science Handbook: Data Mining and Knowledge Discovery Handbook*, pp. 353–374.
- BAUMEISTER, C., AND J. D. HAMILTON (2015): “Sign restrictions, structural vector autoregressions, and useful prior information,” *Econometrica*, 83(5), 1963–1999.
- BENGIO, Y., A. COURVILLE, AND P. VINCENT (2013): “Representation Learning: A Review and New Perspectives,” *IEEE Transactions on Pattern Analysis and Machine Intelligence*, 35(8), 1798–1828.
- BERNANKE, B. S., J. BOIVIN, AND P. ELIASZ (2005): “Measuring the effects of monetary policy: A factor-augmented vector autoregressive (FAVAR) approach,” *The Quarterly Journal of Economics*, 120(1), 387–422.
- BLOOM, N. (2009): “The impact of uncertainty shocks,” *Econometrica*, 77(3), 623–685.
- BLUWSTEIN, K., M. BUCKMANN, A. JOSEPH, S. KAPADIA, AND Ö. ŞİMŞEK (2023): “Credit growth, the yield curve and financial crisis prediction: Evidence from a machine learning approach,” *Journal of International Economics*, p. 103773.
- BOIVIN, J., M. P. GIANNONI, AND I. MIHOV (2009): “Sticky prices and monetary policy: Evidence from disaggregated US data,” *American Economic Review*, 99(1), 350–84.
- BORUP, D., P. G. COULOMBE, D. RAPACH, E. C. M. SCHÜTTE, AND S. SCHWENK-NEBBE (2022): “The anatomy of out-of-sample forecasting accuracy,” .
- CABANILLA, K. I., AND K. T. GO (2019): “Forecasting, Causality, and Impulse Response with Neural Vector Autoregressions,” *arXiv preprint arXiv:1903.09395*.
- CARRIERO, A., J. CHAN, T. E. CLARK, AND M. MARCELLINO (2022a): “Corrigendum to “Large Bayesian vector autoregressions with stochastic volatility and non-conjugate priors” [J. Econometrics 212 (1)(2019) 137–154],” *Journal of Econometrics*, 227(2), 506–512.
- CARRIERO, A., T. E. CLARK, AND M. MARCELLINO (2018): “Measuring uncertainty and its impact on the economy,” *Review of Economics and Statistics*, 100(5), 799–815.
- (2019): “Large Bayesian vector autoregressions with stochastic volatility and non-conjugate priors,” *Journal of Econometrics*, 212(1), 137–154.
- CARRIERO, A., T. E. CLARK, M. MARCELLINO, AND E. MERTENS (2022b): “Addressing COVID-19 outliers in BVARs with stochastic volatility,” *Review of Economics and Statistics*, pp. 1–38.
- CARRIERO, A., T. E. CLARK, M. G. MARCELLINO, AND E. MERTENS (2021): “Measuring uncertainty and its effects in the COVID-19 era,” *CEPR Discussion Paper No. DP15965*.
- CARRIERO, A., H. MUMTAZ, K. THEODORIDIS, AND A. THEOPHILOPOULOU (2015): “The impact of uncertainty shocks under measurement error: A proxy SVAR approach,” *Journal of Money, Credit and Banking*, 47(6), 1223–1238.
- CASCALDI-GARCIA, D. (2022): “Pandemic priors,” *International Finance Discussion Paper*, (1352).
- CHAKRABORTY, C., AND A. JOSEPH (2017): “Machine learning at central banks,” Bank of England Working Papers 674, Bank of England.
- CHRISTIANO, L. J., M. EICHENBAUM, AND C. L. EVANS (2005): “Nominal rigidities and the dynamic effects of a shock to monetary policy,” *Journal of Political Economy*, 113(1), 1–45.
- COULOMBE, P. G. (2020): “The Macroeconomy as a Random Forest,” *arXiv preprint arXiv:2006.12724*.
- COULOMBE, P. G., AND M. GOEBEL (2023): “Maximally Machine-Learnable Portfolios,” *arXiv preprint arXiv:2306.05568*.
- COULOMBE, P. G., M. LEROUX, D. STEVANOVIC, AND S. SURPRENANT (2019): “How is Machine Learning Useful for Macroeconomic Forecasting?,” CIRANO Working Papers 2019s-22, CIRANO.
- COVERT, I., AND S.-I. LEE (2021): “Improving kernelshap: Practical shapley value estimation using linear regression,” in *International Conference on Artificial Intelligence and Statistics*, pp. 3457–3465. PMLR.
- CRAWFORD, L., S. R. FLAXMAN, D. E. RUNCIE, AND M. WEST (2019): “Variable prioritization in nonlinear black box methods: A genetic association case study,” *The Annals of Applied Statistics*, 13(2), 958.
- CRAWFORD, L., K. C. WOOD, X. ZHOU, AND S. MUKHERJEE (2018): “Bayesian approximate kernel regression with variable selection,” *Journal of the American Statistical Association*, 113(524), 1710–1721.
- DAMJANOVIC, M., AND I. MASTEN (2016): “Shadow short rate and monetary policy in the Euro area,” *Empirica*, 43, 279–298.
- DIXON, M. F., AND N. G. POLSON (2019): “Deep Fundamental Factor Models,” *arXiv preprint arXiv:1903.07677*.

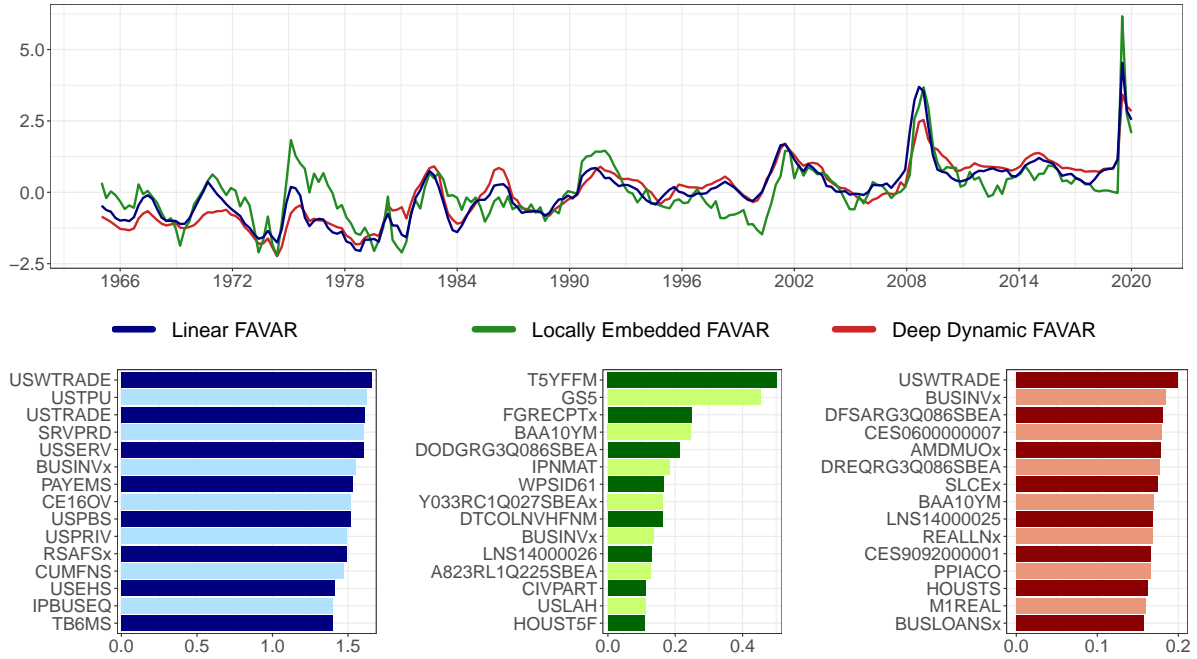
- DOAN, T., R. LITTERMAN, AND C. SIMS (1984): “Forecasting and conditional projection using realistic prior distributions,” *Econometric Reviews*, 3(1), 1–100.
- EICKMEIER, S., W. LEMKE, AND M. MARCELLINO (2015): “Classical time varying factor-augmented vector auto-regressive models—estimation, forecasting and structural analysis,” *Journal of the Royal Statistical Society. Series A (Statistics in Society)*, pp. 493–533.
- ELLIS, C., H. MUMTAZ, AND P. ZABCZYK (2014): “What lies beneath? A time-varying FAVAR model for the UK transmission mechanism,” *The Economic Journal*, 124(576), 668–699.
- FARRELL, M. H., T. LIANG, AND S. MISRA (2018): “Deep neural networks for estimation and inference,” *arXiv preprint arXiv:1809.09953*.
- FENG, G., J. HE, AND N. G. POLSON (2018a): “Deep Learning for Predicting Asset Returns,” *ArXiv*, abs/1804.09314.
- FENG, G., J. HE, N. G. POLSON, AND J. XU (2018b): “Deep learning in characteristics-sorted factor models,” *arXiv preprint arXiv:1805.01104*.
- GALLANT, A. R., AND H. WHITE (1992): “Original Contribution: On Learning the Derivatives of an Unknown Mapping with Multilayer Feedforward Networks,” *Neural Networks*, 5(1), 129 – 138.
- GERTLER, M., AND P. KARADI (2015): “Monetary policy surprises, credit costs, and economic activity,” *American Economic Journal: Macroeconomics*, 7(1), 44–76.
- GIANNONE, D., M. LENZA, AND G. E. PRIMICERI (2015): “Prior selection for vector autoregressions,” *Review of Economics and Statistics*, 97(2), 436–451.
- GLOROT, X., A. BORDES, AND Y. BENGIO (2011): “Deep Sparse Rectifier Neural Networks,” in *Proceedings of the Fourteenth International Conference on Artificial Intelligence and Statistics*, ed. by G. Gordon, D. Dunson, and M. Dudík, vol. 15 of *Proceedings of Machine Learning Research*, pp. 315–323, Fort Lauderdale, FL, USA. JMLR Workshop and Conference Proceedings.
- GNEITING, T., AND A. E. RAFTERY (2007): “Strictly proper scoring rules, prediction, and estimation,” *Journal of the American Statistical Association*, 102(477), 359–378.
- GOODFELLOW, I., Y. BENGIO, AND A. COURVILLE (2016): *Deep Learning*. MIT Press, <http://www.deeplearningbook.org>.
- HAUZENBERGER, N., F. HUBER, AND K. KLIEBER (2020): “Real-time Inflation Forecasting Using Non-linear Dimension Reduction Techniques,” *arXiv preprint arXiv:2012.08155*.
- HAUZENBERGER, N., F. HUBER, K. KLIEBER, AND M. MARCELLINO (2022): “Enhanced Bayesian Neural Networks for Macroeconomics and Finance,” *arXiv preprint arXiv:2211.04752*.
- HE, X., D. CAI, S. YAN, AND H.-J. ZHANG (2005): “Neighborhood preserving embedding,” in *Tenth IEEE International Conference on Computer Vision (ICCV’05) Volume 1*, vol. 2, pp. 1208–1213. IEEE.
- HEATON, J. (2008): *Introduction to neural networks with Java*. Heaton Research, Inc.
- HEATON, J. B., N. G. POLSON, AND J. H. WITTE (2017): “Deep learning for finance: deep portfolios,” *Applied Stochastic Models in Business and Industry*, 33(1), 3–12.
- HORNIK, K. (1991): “Approximation capabilities of multilayer feedforward networks,” *Neural Networks*, 4(2), 251–257.
- HORNIK, K., M. STINCHCOMBE, AND H. WHITE (1989): “Multilayer feedforward networks are universal approximators,” *Neural Networks*, 2(5), 359–366.
- HUBER, F., AND M. M. FISCHER (2018): “A Markov switching factor-augmented VAR model for analyzing US business cycles and monetary policy,” *Oxford Bulletin of Economics and Statistics*, 80(3), 575–604.
- HUBER, F., G. KOOP, L. ONORANTE, M. PFARRHOFER, AND J. SCHREINER (2020): “Nowcasting in a pandemic using non-parametric mixed frequency VARs,” *Journal of Econometrics*, (forthcoming).
- JOSEPH, A., G. POTJAGAILO, E. KALAMARA, C. CHAKRABORTY, AND G. KAPETANIOS (2021): “Forecasting UK inflation bottom up,” .
- JURADO, K., S. C. LUDVIGSON, AND S. NG (2015): “Measuring uncertainty,” *American Economic Review*, 105(3), 1177–1216.
- KASTNER, G., AND S. FRÜHWIRTH-SCHNATTER (2014): “Ancillarity-sufficiency interweaving strategy (ASIS) for boosting MCMC estimation of stochastic volatility models,” *Computational Statistics & Data Analysis*, 76(C), 408–423.
- KAYO, O. (2006): “LOCALLY LINEAR EMBEDDING ALGORITHM—Extensions and applications,” .
- KELLY, B., S. PRUITT, AND Y. SU (2018): “Characteristics Are Covariances: A Unified Model of Risk and Return,” Working Paper 24540, National Bureau of Economic Research.
- KILIAN, L., AND H. LÜTKEPOHL (2017): *Structural vector autoregressive analysis*. Cambridge University Press.
- KING, R. G., C. I. PLOSSER, J. H. STOCK, AND M. W. WATSON (1991): “Stochastic Trends and Economic Fluctuations,” *The American Economic Review*, pp. 819–840.
- KOOP, G., AND D. KOROBILIS (2014): “A new index of financial conditions,” *European Economic Review*, 71, 101–116.
- KOROBILIS, D. (2013): “Assessing the transmission of monetary policy using time-varying parameter dynamic factor models,” *Oxford Bulletin of Economics and Statistics*, 75(2), 157–179.
- LANNE, M., AND H. LÜTKEPOHL (2008): “Identifying monetary policy shocks via changes in volatility,” *Journal of Money, Credit and Banking*, 40(6), 1131–1149.
- (2010): “Structural vector autoregressions with nonnormal residuals,” *Journal of Business & Economic Statistics*, 28(1), 159–168.

- LENZA, M., AND G. E. PRIMICERI (2020): “How to estimate a VAR after March 2020,” Discussion paper, National Bureau of Economic Research.
- LOMBARDI, M., AND F. ZHU (2018): “A Shadow Policy Rate to Calibrate US Monetary Policy at the Zero Lower Bound,” *International Journal of Central Banking*, 14(5), 305–346.
- LUNDBERG, S. M., AND S.-I. LEE (2017): “A unified approach to interpreting model predictions,” *Advances in Neural Information Processing Systems*, 30.
- LÜTKEPOHL, H., AND T. WOŹNIAK (2020): “Bayesian inference for structural vector autoregressions identified by Markov-switching heteroskedasticity,” *Journal of Economic Dynamics and Control*, 113, 103862.
- MARCELLINO, M. (2006): “Leading indicators,” *Handbook of Economic Forecasting*, 1, 879–960.
- MCCRACKEN, M., AND S. NG (2020): “FRED-QD: A quarterly database for macroeconomic research,” Discussion paper, National Bureau of Economic Research.
- MERTENS, K., AND M. O. RAVN (2013): “The dynamic effects of personal and corporate income tax changes in the United States,” *American Economic Review*, 103(4), 1212–47.
- MULLAINATHAN, S., AND J. SPIESS (2017): “Machine Learning: An Applied Econometric Approach,” *Journal of Economic Perspectives*, 31(2), 87–106.
- NG, S. (2021): “Modeling Macroeconomic Variations after Covid-19,” *NBER Working Paper*, (w29060).
- PAGAN, A. R., AND M. H. PESARAN (2008): “Econometric analysis of structural systems with permanent and transitory shocks,” *Journal of Economic Dynamics and Control*, 32(10), 3376–3395.
- POTJAGAILO, G. (2017): “Spillover effects from Euro area monetary policy across Europe: A factor-augmented VAR approach,” *Journal of International Money and Finance*, 72, 127–147.
- PRIMICERI, G. E., AND A. TAMBALOTTI (2020): “Macroeconomic Forecasting in the Time of COVID-19,” *Manuscript, Northwestern University*, pp. 1–23.
- RIGOBON, R. (2003): “Identification through heteroskedasticity,” *Review of Economics and Statistics*, 85(4), 777–792.
- ROWEIS, S. T., AND L. K. SAUL (2000): “Nonlinear dimensionality reduction by locally linear embedding,” *Science*, 290(5500), 2323–2326.
- SCHORFHEIDE, F., AND D. SONG (2020): “Real-Time Forecasting with a (Standard) Mixed-Frequency VAR During a Pandemic,” Working Papers 20-26, Federal Reserve Bank of Philadelphia.
- SHAPLEY, L. S. (1953): “A value for n-person games,” *Contributions to the Theory of Games*, pp. 307–317.
- SIMS, C. A., AND T. ZHA (1998): “Bayesian methods for dynamic multivariate models,” *International Economic Review*, pp. 949–968.
- STOCK, J., AND M. WATSON (2002): “Macroeconomic forecasting using diffusion indexes,” *Journal of Business & Economic Statistics*, 20(2), 147–162.
- STOCK, J. H., AND M. W. WATSON (1989): “New indexes of coincident and leading economic indicators,” *NBER Macroeconomics Annual*, 4, 351–394.
- (2005): “Implications of dynamic factor models for VAR analysis,” Discussion paper, National Bureau of Economic Research.
- STRUMBELJ, E., AND I. KONONENKO (2010): “An efficient explanation of individual classifications using game theory,” *The Journal of Machine Learning Research*, 11, 1–18.
- THEODORIDIS, S. (2015): *Machine learning: a Bayesian and optimization perspective*. Academic Press.
- UHLIG, H. (2005): “What are the effects of monetary policy on output? Results from an agnostic identification procedure,” *Journal of Monetary Economics*, 52(2), 381–419.
- WANG, Y., A. SMOLA, D. MADDIX, J. GASTHAUS, D. FOSTER, AND T. JANUSCHOWSKI (2019): “Deep factors for forecasting,” in *International conference on machine learning*, pp. 6607–6617. PMLR.
- WU, J. C., AND F. D. XIA (2016): “Measuring the macroeconomic impact of monetary policy at the zero lower bound,” *Journal of Money, Credit and Banking*, 48(2-3), 253–291.

Appendices

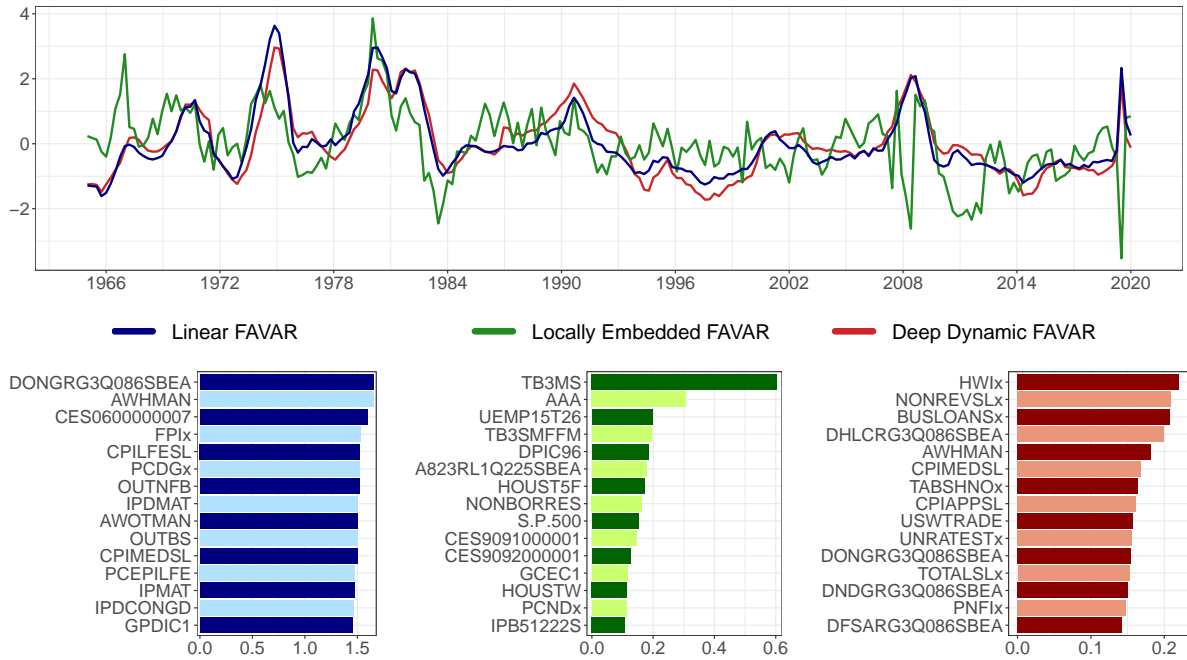
A Additional results

Figure 10: First latent factor arising from linear and non-linear dimension reduction techniques and corresponding variable importance for 2020Q4.



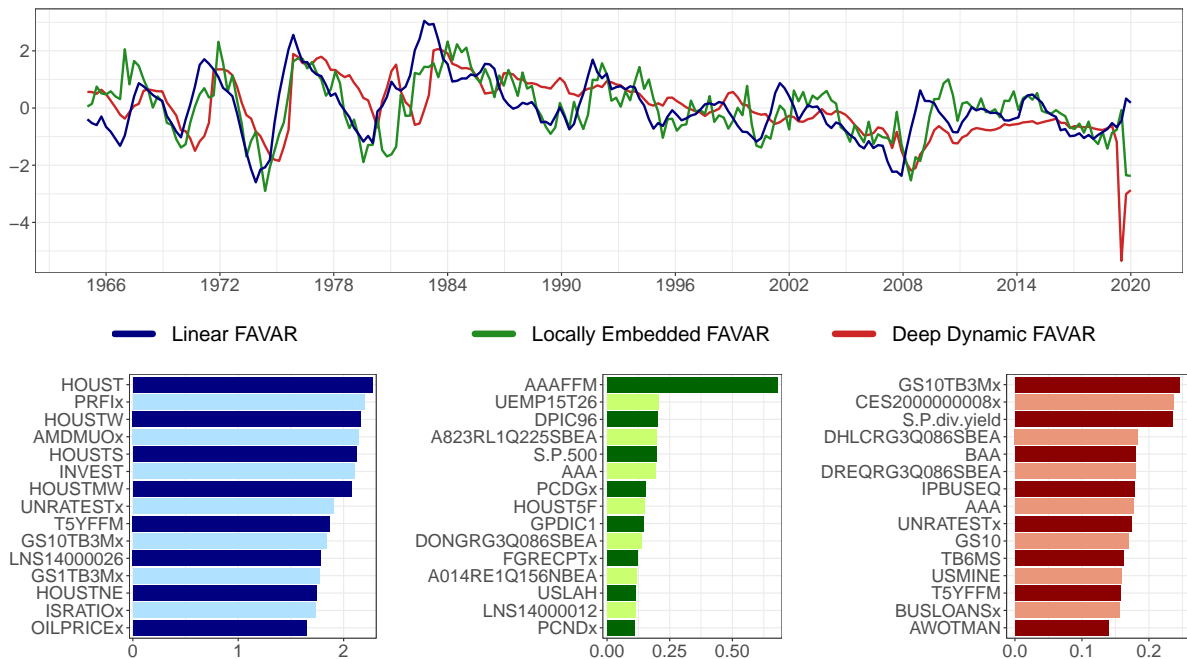
Note: The upper panel depicts normalized factors of the three dimension reduction techniques (mapped according to the highest correlation) with mean zero and variance one obtained from the main dataset ($N = 162$) ranging from 1965Q1 to 2020Q4. The barplots show the 15 most important variables for each factor measured by the factor loadings for the linear FAVAR and the Locally Embedded FAVAR and Shapley values for the Deep Dynamic FAVAR. Mnemonics are those of McCracken and Ng (2020) and can be found in Appendix C.

Figure 11: Second latent factor arising from linear and non-linear dimension reduction techniques and corresponding variable importance for 2020Q4.



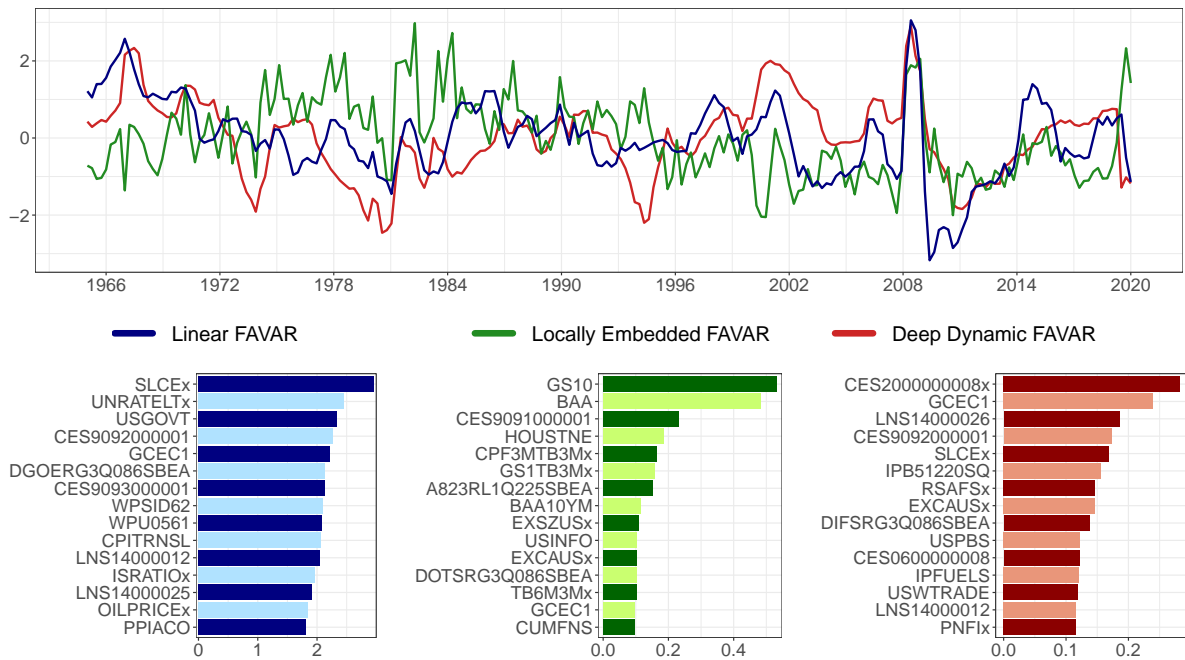
Note: For more details I refer to Figure 10.

Figure 12: Third latent factor arising from linear and non-linear dimension reduction techniques and corresponding variable importance for 2020Q4.



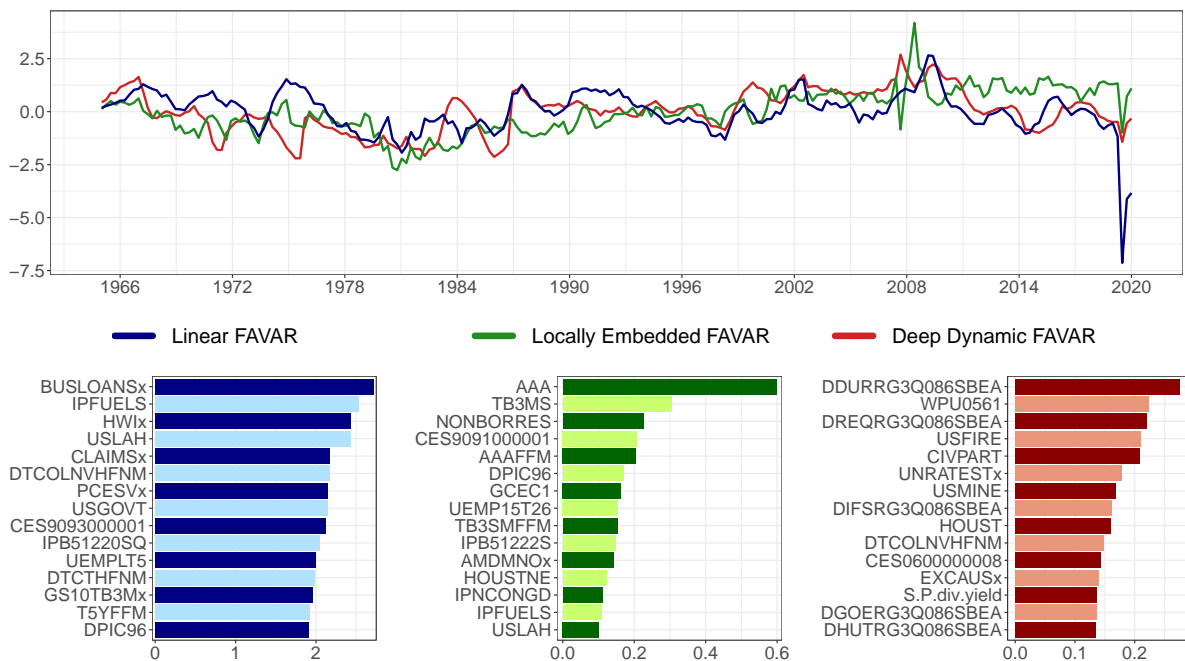
Note: For more details I refer to Figure 10.

Figure 13: Fourth latent factor arising from linear and non-linear dimension reduction techniques and corresponding variable importance for 2020Q4.



Note: For more details I refer to Figure 10.

Figure 14: Fifth latent factor arising from linear and non-linear dimension reduction techniques and corresponding variable importance for 2020Q4.



Note: For more details I refer to Figure 10.

Table 3: Relative point and density forecasting performance for simulated data

Variables	Crisis Times		Tranquil Times	
	RMSE	CRPS	RMSE	CRPS
Deep Dynamic FAVAR				
Variable 1	0.94	0.92	1.00	1.00
Variable 2	0.89	0.87	1.03	1.01
Variable 3	0.83	0.78	1.03	1.02
Variable 4	0.84	0.84	0.97	0.99
Variable 5	0.93	0.92	0.98	0.99
Variable 6	0.95	0.96	0.99	0.99
Variable 7	0.79	0.75	1.00	0.99
Variable 8	0.72	0.67	0.98	0.99
Variable 9	0.86	0.84	1.00	0.99
Variable 10	1.02	1.00	1.09	1.04
Variable 11	0.72	0.66	0.96	0.97
Variable 12	1.05	1.08	1.03	1.01
Variable 13	1.12	1.16	1.05	1.01
Variable 14	1.08	1.17	1.04	1.01
Variable 15	1.11	1.15	1.02	1.00
Variable 16	0.90	0.89	1.03	1.01
Variable 17	0.85	0.87	0.98	0.99
Variable 18	0.78	0.77	0.97	0.99
Variable 19	0.98	1.04	0.98	0.99
Variable 20	1.05	1.02	1.16	1.11
Locally Embedded FAVAR				
Variable 1	1.02	1.03	1.00	1.00
Variable 2	0.95	0.94	1.00	1.00
Variable 3	0.97	0.97	1.00	1.01
Variable 4	0.96	0.95	0.99	1.00
Variable 5	1.03	1.04	1.00	1.00
Variable 6	0.97	0.96	0.99	1.00
Variable 7	0.99	0.98	1.01	1.00
Variable 8	0.94	0.94	0.99	1.00
Variable 9	1.00	1.01	1.00	1.00
Variable 10	0.99	0.99	1.01	1.01
Variable 11	1.01	1.01	0.99	1.00
Variable 12	1.01	1.01	0.99	1.00
Variable 13	1.00	0.99	1.01	1.01
Variable 14	0.97	0.98	0.99	1.00
Variable 15	1.01	1.01	1.00	1.00
Variable 16	0.99	0.98	1.00	1.00
Variable 17	0.98	0.98	0.99	1.00
Variable 18	0.99	0.99	1.00	1.00
Variable 19	0.97	0.98	0.99	1.00
Variable 20	0.99	0.98	1.02	1.03

Note: The table shows point forecasting performance in terms of root mean squared errors (RMSE) as well as density forecasting performance in terms of continuous ranked probability scores (CRPS). All metrics are relative to the linear FAVAR. Values below one (bold numbers) show that the non-linear model outperforms the linear one.

B Technical Appendix

B.1 Equation-by-equation estimation

Before I sketch the implemented prior in more detail, I briefly discuss the equation-by-equation estimation approach. As shown by [Carriero et al. \(2019, 2022a\)](#), one can exploit the fact that $\Sigma_\epsilon = \tilde{\mathbf{A}}_0^{-1} \Sigma_{\tilde{\epsilon}} \tilde{\mathbf{A}}_0^{-1'}$ with $\tilde{\mathbf{A}}_0^{-1}$ being a lower triangular matrix and $\Sigma_{\tilde{\epsilon}}$ being diagonal and write the VAR model as K independent regressions. I collect the coefficient matrices in an $K \times 2(Kp+1)$ -dimensional matrix $\mathbf{A} = (\mathbf{A}_1, \dots, \mathbf{A}_p, \mathbf{c})$ and the regressors in an $K \times 1$ -dimensional vector $\mathbf{x}_t = (\mathbf{y}'_{t-1}, \dots, \mathbf{y}'_{t-p}, 1)'$. Moreover, I define $\tilde{\mathbf{y}}_t = \tilde{\mathbf{A}}_0 \mathbf{y}_t$. This allows to rewrite Eq. 2 as

$$\tilde{\mathbf{y}}_t = \tilde{\mathbf{A}}_0 \mathbf{y}_t = \tilde{\mathbf{A}}_0 \mathbf{A} \mathbf{x}_t + \tilde{\epsilon}_t, \quad \tilde{\epsilon}_t \sim \mathcal{N}(\mathbf{0}, \Sigma_{\tilde{\epsilon}})$$

The fact that the variance-covariance matrix $\Sigma_{\tilde{\epsilon}}$ is diagonal allows to write the VAR model as K independent regressions where the first equation in the system is given by

$$\tilde{y}_{1t} = \mathbf{x}'_t \mathbf{A}_{\bullet 1} + \tilde{\epsilon}_{1t}, \quad \tilde{\epsilon}_{1t} \sim \mathcal{N}(0, \tilde{\sigma}_1)$$

with $\mathbf{A}_{\bullet 1}$ depicting the first column in \mathbf{A} and $\tilde{\epsilon}_{1t}$ the first element in $\tilde{\epsilon}_t$. $\tilde{\sigma}_1$ refers to the first diagonal element in $\Sigma_{\tilde{\epsilon}}$. The following k equations for $k = 2, \dots, K$ are given by

$$\begin{aligned} \tilde{y}_{2t} &= \tilde{A}_{0;2,1} \mathbf{x}'_t \mathbf{A}_{\bullet 1} + \mathbf{x}'_t \mathbf{A}_{\bullet 2} + \tilde{\epsilon}_{2t}, \quad \tilde{\epsilon}_{2t} \sim \mathcal{N}(0, \tilde{\sigma}_2) \\ &\vdots \\ \tilde{y}_{Kt} &= \tilde{A}_{0;K,1} \mathbf{x}'_t \mathbf{A}_{\bullet 1} + \dots + \tilde{A}_{0;K,K-1} \mathbf{x}'_t \mathbf{A}_{\bullet K-1} + \mathbf{x}'_t \mathbf{A}_{\bullet K} + \tilde{\epsilon}_{Kt}, \quad \tilde{\epsilon}_{Kt} \sim \mathcal{N}(0, \tilde{\sigma}_K) \end{aligned}$$

where $\mathbf{A}_{\bullet k}$ denotes the k th column in \mathbf{A} and $\tilde{A}_{0,ki}$ is the (k, i) th element in $\tilde{\mathbf{A}}_0$. $\tilde{\sigma}_k$ is the k th diagonal element in $\Sigma_{\tilde{\epsilon}}$ (for $k = 1, \dots, K$).

B.2 Prior structure

For the estimation of the models proposed in this paper I implement the well-known Minnesota prior ([Doan et al., 1984](#); [Sims and Zha, 1998](#)). The main idea is to center the system on a multivariate random walk, which is assumed to reflect the notion of the variables a priori. Furthermore, own lags are assumed to provide more information on the variation of a certain variable than lags of other variables and that the variables becomes less important with increasing lag length.

I assume that each α_k follows a normal distribution

$$\alpha_k \sim \mathcal{N}(\underline{\alpha}_k, \underline{\mathbf{V}}_k)$$

where the corresponding prior mean is denoted by $\underline{\alpha}_k$ and the prior variance-covariance matrix by $\underline{\mathbf{V}}_k$. For stationary series, such as the latent factors and the uncertainty index, I set $\underline{\alpha}_k$ to zero. For non-stationary data, I define $\underline{\alpha}_k = 1$.

The prior variance-covariance matrix $\underline{\mathbf{V}}_k$ is diagonal with the i th diagonal element chosen such that

$$\underline{\mathbf{V}}_{k,ii} = \begin{cases} \frac{\xi_1}{r^2} & \text{on the coefficients of own lags (for } r = 1, \dots, p) \\ \frac{\xi_2 \hat{\sigma}_i^2}{r^2 \hat{\sigma}_j^2} & \text{on the coefficients of other variables' lags (} i \neq j) \\ \xi_3 & \text{on the intercept term.} \end{cases}$$

ξ_1 and ξ_2 denote scaling parameters, which make sure that coefficients are more heavily shrunk to zero with increasing lag length and with $\xi_1 > \xi_2$ that own coefficients are more likely to be important than

those of other variables. ξ_3 controls the prior on the intercept term. We set $\xi_3 = 1000$ and estimate the parameters ξ_1 and ξ_2 within the sampler as suggested by Giannone et al. (2015). $\hat{\sigma}^2$ is determined by estimating the variance of an AR(4) process in $\Delta \mathbf{y}$ via OLS.

B.3 MCMC sampling algorithm

The sampling algorithm is comprised of the following steps:

1. I draw $\boldsymbol{\alpha}_k$ for $k = 1, \dots, K$ from a multivariate Normal distribution

$$\boldsymbol{\alpha}_k \sim \mathcal{N}(\bar{\boldsymbol{\alpha}}_k, \bar{\mathbf{V}}_k)$$

where $\bar{\boldsymbol{\alpha}}_k$ and $\bar{\mathbf{V}}_k$ denote the posterior quantities given by

$$\begin{aligned} \bar{\boldsymbol{\alpha}}_k &= \bar{\mathbf{V}}_k(\tilde{\mathbf{X}}_k' \mathbf{y}_k / \tilde{\sigma}_k + \mathbf{V}_k^{-1} \boldsymbol{\alpha}_k) \\ \bar{\mathbf{V}}_k &= (\tilde{\mathbf{X}}_k' \tilde{\mathbf{X}}_k / \tilde{\sigma}_k + \mathbf{V}_k^{-1})^{-1} \end{aligned}$$

$\boldsymbol{\alpha}_k$ refers to the prior mean $\boldsymbol{\alpha}$ for equation k and \mathbf{V}_k to the prior variance-covariance matrix \mathbf{V} as specified in Section B.2 for equation k .

2. The structural error variances $\tilde{\sigma}_k$ for $k = 1, \dots, K$ are sampled from an inverse Gamma distribution:

$$\tilde{\sigma}_k \sim \mathcal{IG}(e_k, d_k)$$

with $e_k = (T/2 + 0.005)$ and $d_k = (\tilde{\boldsymbol{\epsilon}}_k' \tilde{\boldsymbol{\epsilon}}_k / 2 + 0.005)$.

3. Updating the Minnesota parameters ξ_1 and ξ_2 involves drawing candidate values from a Gaussian distribution with mean $\xi_1^{(jj-1)}$ and $\xi_2^{(jj-1)}$ and variance \tilde{c}_1 and \tilde{c}_2 . $\xi_1^{(jj-1)}$ and $\xi_2^{(jj-1)}$ denote the previous draws of ξ_1 and ξ_2 and \tilde{c}_1 and \tilde{c}_2 are defined as a scaling parameters chosen such that the acceptance rate is between 15 and 30 percent. I update the parameter values with probability $\beta^{(jj)}$ and stick with the previous values with probability $(1 - \beta^{(jj)})$. $\beta^{(jj)}$ is determined by comparing the likelihood of the parameter proposals and the likelihood of the previous parameter values conditional on the data. According to this choice we update $\mathbf{V}_{i,j}$ for the next draw from the posterior distribution. This procedure follows Giannone et al. (2015).

B.4 Variable importance measures for the non-linear FAVARs

Neighborhood Preserving Embedding for the Locally Embedded FAVAR. To get interpretable factor loadings from the locally linear embedding algorithm, I implement the Neighborhood Preserving Embedding of He et al. (2005). After computing the weight matrix $\boldsymbol{\Omega}$ I make use of a linear approximation and assume that $\hat{\mathbf{F}} = \mathbf{P}' \mathbf{D}$. This changes the cost function for $\hat{\mathbf{F}}$ for being the new data point in Eq. 5 to

$$\Phi(\hat{\mathbf{F}}) = \sum_i |\mathbf{P}' \mathbf{d}_{\bullet i} - \sum_j \Omega_{ij} \mathbf{P}' \mathbf{d}_{\bullet j}|^2$$

The last step is then to solve the standard eigenvalue problem given by

$$\mathbf{D} \mathbf{M} \mathbf{D}' \mathbf{P} = \mathbf{D} \mathbf{D}' \mathbf{P} \boldsymbol{\Lambda}$$

with $\mathbf{M} = (\mathbf{I}_t + \boldsymbol{\Omega})' (\mathbf{I}_t + \boldsymbol{\Omega})$ and $\boldsymbol{\Lambda}$ denoting the eigenvalue matrix with diagonal elements being the eigenvalues of $(\mathbf{D} \mathbf{D}')^{-1} \mathbf{D} \mathbf{M} \mathbf{D}'$. Similar to PCA this can be solved by applying Singular Value Decomposition (SVD) and the resulting factors enjoy interpretability via the factor loadings.

Shapley values for the Deep Dynamic FAVAR. Machine learning techniques, such as the autoencoder, are very flexible approaches but often face the criticism of being hard to interpret. To tackle the black box critique the variable importance measure for the Deep Dynamic FAVAR is based on the Shapley additive explanations framework (Strumbelj and Kononenko, 2010; Lundberg and Lee, 2017), which is itself inspired from the concept of Shapley values (Shapley, 1953). The recent macro and finance literature shows growing interest in this type of measures to gain interpretable results of highly non-linear techniques (see, Joseph et al., 2021; Borup et al., 2022; Bluwstein et al., 2023; Coulombe and Goebel, 2023). In the proposed framework, it allows to identify the key drivers of the deep dynamic factors and give them some basic economic meaning.

Let $\phi_{t,k}$ be the Shapley value at time t (for $t = 1, \dots, T$) and variable k (for $k = 1, \dots, K$). Each predicted factor $\hat{F}_{t,q}$ (for $q = 1, \dots, Q$) can be decomposed into

$$\hat{F}_{t,q} = \sum_{k=1}^K \phi_{t,k} + \phi_0,$$

where ϕ_0 is the mean predicted value in the training set and can be interpreted as an intercept. Computing the Shapley value of each variable k involves deriving its marginal contribution to the prediction of the factor. This is done by comparing the payoffs of all possible coalitions of regressors, formally given by

$$\phi_{t,k} = \sum_{\mathcal{S} \subseteq K/k} \frac{S!(K-S-1)!}{K!} (f(\mathcal{S} \cup \{k\}) - f(\mathcal{S})),$$

with the payoff of a coalition $\mathcal{S} \subseteq K$ denoted by $f(\mathcal{S})$ and the payoff of the same coalition combined with regressor k being $f(\mathcal{S} \cup \{k\})$. The difference between these two measures gives the marginal contribution of variable k to the coalition. Since the computational burden of Shapley values for large datasets is considerable, an almost exact hybrid algorithm of Covert and Lee (2021) is used.

C Data Appendix

The Federal Reserve Economic Data (FRED) contains quarterly observations of macroeconomic variables for the US and is available for download at <https://research.stlouisfed.org>. Details on the dataset can be found in [McCracken and Ng \(2020\)](#). The time series start from 1959 Q1 and encompasses 248 quarterly series in total. Due to missing values, I preselect 166 variables starting from 1965 Q1 covering all sectors of the economy and transform them according to [Table B.2](#). The last column in [Table B.2](#) classifies the variables into slow- and fast-moving quantities for the identification by zero restrictions on contemporaneous effects.

For the determination of the average duration of the US business cycle I use the data provided by the National Bureau of Economic Research downloadable at <https://www.nber.org/research/data/us-business-cycle-expansions-and-contractions>. I consider 12 cycles between 1945 and 2020 with an average duration of 75 months from peak to peak, i.e. six years.

Table B.1: Data description

FRED.Mnemonic	Description	Trans.	Obs. var.	Type
GDPC1	Real Gross Domestic Product	50		slow
PCECC96	Real Personal Consumption Expenditures	50		slow
PCDGx	Real personal consumption expenditures: Durable goods	50		slow
PCESVx	Real Personal Consumption Expenditures: Services	50		slow
PCNDx	Real Personal Consumption Expenditures: Nondurable Goods	50		slow
GPDIC1	Real Gross Private Domestic Investment	50		slow
FPIx	Real private fixed investment	50		slow
Y033RC1Q027SBEAx	Real Gross Private Domestic Investment: Fixed Investment: Nonresidential Equip	50		slow
PNFIx	Real private fixed investment: Nonresidential	50		slow
PRFIx	Real private fixed investment: Residential	50		slow
A014RE1Q156NBEA	Shares of gross domestic product: Change in private inventories	1		slow
GCEC1	Real Government Consumption Expenditures and Gross Investment	50		slow
A823RL1Q225SBEA	Real Government Consumption Expenditures and Gross Investment: Federal	1		slow
FGRECPTx	Real Federal Government Current Receipts	50		slow
SLCEx	Real government state and local consumption expenditures	50		slow
EXPGSC1	Real Exports of Goods and Services	50		slow
IMPGSC1	Real Imports of Goods and Services	50		slow
DPIC96	Real Disposable Personal Income	50		slow
OUTNFB	Nonfarm Business Sector: Real Output	50		slow
OUTBS	Business Sector: Real Output	50		slow
INDPRO	IP:Total index Industrial Production Index (Index 2012=100)	50	x	slow
IPFINAL	IP:Final products Industrial Production (Market Group) (Index 2012=100)	50		slow
IPCONGD	IP:Consumer goods Industrial Production: Consumer Goods (Index 2012=100)	50		slow
IPMAT	Materials (Index 2012=100)	50		slow
IPDMAT	Durable Materials (Index 2012=100)	50		slow
IPNMAT	Nondurable Materials (Index 2012=100)	50		slow
IPDCONGD	Durable Consumer Goods (Index 2012=100)	50		slow
IPB51110SQ	Durable Goods: Automotive products (Index 2012=100)	50		slow
IPNCONGD	Nondurable Consumer Goods (Index 2012=100)	50		slow
IPBUSEQ	Business Equipment (Index 2012=100)	50		slow
IPB51220SQ	Consumer energy products (Index 2012=100)	50		slow
CUMFNS	Capacity Utilization: Manufacturing (SIC) (Percent of Capacity)	1		slow
IPMANSICS	Industrial Production: Manufacturing (SIC) (Index 2012=100)	50		slow
IPB51222S	Industrial Production: Residential Utilities (Index 2012=100)	50		slow
IPFUELS	Industrial Production: Fuels (Index 2012=100)	50		slow
PAYEMS	Emp:Nonfarm All Employees: Total nonfarm (Thousands of Persons)	50		slow
USPRIV	All Employees: Total Private Industries (Thousands of Persons)	50		slow
MANEMP	All Employees: Manufacturing (Thousands of Persons)	50		slow
SRVPRD	All Employees: Service-Providing Industries (Thousands of Persons)	50		slow
USGOOD	All Employees: Goods-Producing Industries (Thousands of Persons)	50		slow
DMANEMP	All Employees: Durable goods (Thousands of Persons)	50		slow
NDMANEMP	All Employees: Nondurable goods (Thousands of Persons)	50		slow
USCONS	All Employees: Construction (Thousands of Persons)	50		slow
USEHS	All Employees: Education & Health Services (Thousands of Persons)	50		slow
USFIRE	All Employees: Financial Activities (Thousands of Persons)	50		slow
USINFO	All Employees: Information Services (Thousands of Persons)	50		slow
USPBS	All Employees: Professional & Business Services (Thousands of Persons)	50		slow
USLAH	All Employees: Leisure & Hospitality (Thousands of Persons)	50		slow
USSERV	All Employees: Other Services (Thousands of Persons)	50		slow
USMINE	All Employees: Mining and logging (Thousands of Persons)	50		slow
USTPU	All Employees: Trade, Transportation & Utilities (Thousands of Persons)	50		slow
USGOVT	All Employees: Government (Thousands of Persons)	50		slow
USTRADE	All Employees: Retail Trade (Thousands of Persons)	50		slow
USWTRADE	All Employees: Wholesale Trade (Thousands of Persons)	50		slow
CES9091000001	All Employees: Government: Federal (Thousands of Persons)	50		slow
CES9092000001	All Employees: Government: State Government (Thousands of Persons)	50		slow
CES9093000001	All Employees: Government: Local Government (Thousands of Persons)	50		slow
CE16OV	Civilian Employment (Thousands of Persons)	50		slow
CIVPART	Civilian Labor Force Participation Rate (Percent)	1		slow
UNRATE	Civilian Unemployment Rate (Percent)	1	x	slow
UNRATESTx	Unemployment Rate less than 27 weeks (Percent)	1		slow
UNRATELTx	Unemployment Rate for more than 27 weeks (Percent)	1		slow
LNS14000012	Unemployment Rate - 16 to 19 years (Percent)	1		slow
LNS14000025	Unemployment Rate - 20 years and over, Men (Percent)	1		slow
LNS14000026	Unemployment Rate - 20 years and over, Women (Percent)	1		slow
UEMPLT5	Number of Civilians Unemployed - Less Than 5 Weeks (Thousands of Persons)	50		slow
UEMP5TO14	Number of Civilians Unemployed for 5 to 14 Weeks (Thousands of Persons)	50		slow
UEMP15T26	Number of Civilians Unemployed for 15 to 26 Weeks (Thousands of Persons)	50		slow
UEMP27OV	Number of Civilians Unemployed for 27 Weeks and Over (Thousands of Persons)	50		slow
AWHMAN	Average Weekly Hours of Prod and Nonsuperv Employees: Manufacturing	1		slow
AWOTMAN	Avg Weekly Overtime Hours of Prod and NonsupervEmployees: Manufacturing	1		slow
HWIx	Help-Wanted Index	1		slow
CES0600000007	Average Weekly Hours of Prod and NonsupervEmployees: Goods-Producing	1		slow
CLAIMSx	Initial Claims	50		slow
HOUST	Housing Starts: Total: New Privately Owned Housing Units Started	50		slow
HOUST5F	Privately Owned Housing Starts: 5-Unit Structures or More	50		slow
PERMIT	New Private Housing Units Authorized by Building Permits	50		slow
HOUSTMW	Housing Starts in Midwest Census Region (Thousands of Units)	50		slow
HOUSTNE	Housing Starts in Northeast Census Region (Thousands of Units)	50		slow
HOUSTS	Housing Starts in South Census Region (Thousands of Units)	50		slow
HOUSTW	Housing Starts in West Census Region (Thousands of Units)	50		slow
RSAFSx	Real Retail and Food Services Sales (Millions of Chained 2012 Dollars)	50		slow
AMDMNOx	Real Manufacturers New Orders: Durable Goods (Millions of 2012 Dollars)	50		slow
AMDMUOx	Real Value of Manufacturers Unfilled Orders for Durable Goods Industries	50		slow

Data description (cont.)

FRED.Mnemonic	Description	Trans.	Obs. var.	Type
BUSINVx	Total Business Inventories (Millions of Dollars)	50		slow
ISRATIOx	Total Business: Inventories to Sales Ratio	1		slow
PCECTPI	Pers Cons Exp: Chain-type Price Index	50		slow
PCEPILFE	Personal Consumption Expenditures Excluding Food and Energy	50		slow
GDPCCTPI	Gross Domestic Product: Chain-type Price Index	50		slow
GPDICTPI	Gross Private Domestic Investment: Chain-type Price Index	50		slow
IPDBS	Business Sector: Implicit Price Deflator (Index 2012=100)	50		slow
DGDSRG3Q086SBEA	Pers Cons Exp: Goods	50		slow
DDURRG3Q086SBEA	Pers Cons Exp: Durable goods	50		slow
DSERRG3Q086SBEA	Pers Cons Exp: Services	50		slow
DNDGRG3Q086SBEA	Pers Cons Exp: Nondurable goods	50		slow
DHCERG3Q086SBEA	Pers Cons Exp: Services: Household consumption expenditures	50		slow
DMOTRG3Q086SBEA	Pers Cons Exp: Durable goods: Motor vehicles and parts	50		slow
DFDHRG3Q086SBEA	Pers Cons Exp: Durable goods: Furnishings and durable household equipment	50		slow
DREQRG3Q086SBEA	Pers Cons Exp: Durable goods: Recreational goods and vehicles	50		slow
DODGRG3Q086SBEA	Pers Cons Exp: Durable goods: Other durable goods	50		slow
DFXARG3Q086SBEA	Pers Cons Exp: Nondurable goods: Food and beverages for off-premises cons	50		slow
DCLOGRG3Q086SBEA	Pers Cons Exp: Nondurable goods: Clothing and footwear	50		slow
DGOERG3Q086SBEA	Pers Cons Exp: Nondurable goods: Gasoline and other energy goods	50		slow
DONGRG3Q086SBEA	Pers Cons Exp: Nondurable goods: Other nondurable goods	50		slow
DHUTRG3Q086SBEA	Pers Cons Exp: Services: Housing and utilities	50		slow
DHLCRG3Q086SBEA	Pers Cons Exp: Services: Health care	50		slow
DTRSrg3Q086SBEA	Pers Cons Exp: Transportation services	50		slow
DRCARG3Q086SBEA	Pers Cons Exp: Recreation services	50		slow
DFSARG3Q086SBEA	Pers Cons Exp: Services: Food services and accomodations	50		slow
DIFSrg3Q086SBEA	Pers Cons Exp: Financial services and insurance	50		slow
DOTSRG3Q086SBEA	Pers Cons Exp: Other services	50		slow
CPIAUCSL	Consumer Price Index for All Urban Consumers: All Items	50	x	slow
CPILFESL	Consumer Price Index for All Urban Consumers: All Items Less Food & Energy	50		slow
WPSFD49207	Producer Price Index by Commodity for Finished Goods	50		slow
PPIACO	Producer Price Index for All Commodities	50		slow
WPSFD49502	Producer Price Index by Commodity for Finished Consumer Goods	50		slow
WPSFD4111	Producer Price Index by Commodity for Finished Consumer Foods	50		slow
PII1DC	Producer Price Index by Commodity Industrial Commodities	50		slow
WPSID61	PPI by Commodity Intermediate Materials: Supplies & Components	50		slow
WPU0561	Producer Price Index by Commodity for Fuels and Related Products and Power	50		slow
OILPRICEx	Real Crude Oil Prices: West Texas Intermediate (WTI) - Cushing, Oklahoma	50		slow
WPSID62	Producer Price Index: Crude Materials for Further Processing	50		slow
PPICMM	PPI: Commodities: Metals and metal products: Primary nonferrous metals	50		slow
CPIAPPSL	Consumer Price Index for All Urban Consumers: Apparel	50		slow
CPITRNSL	Consumer Price Index for All Urban Consumers: Transportation	50		slow
CPIMEDSL	Consumer Price Index for All Urban Consumers: Medical Care	50		slow
CUSR0000SAC	Consumer Price Index for All Urban Consumers: Commodities	50		slow
CES2000000008x	Real Average Hourly Earnings of Prod and Nonsuperv Employees: Construction	50		slow
CES3000000008x	Real Average Hourly Earnings of Prod and Nonsuperv Employees: Manufacturing	50		slow
COMPRNFB	Nonfarm Business Sector: Real Compensation Per Hour (Index 2012=100)	50		slow
CES0600000008	Average Hourly Earnings of Production and Nonsupervisory Employees:	50		slow
Shadow Rate	Shadow Federal Funds Rate (Percent)	1	x	policy
TB3MS	3-Month Treasury Bill: Secondary Market Rate (Percent)	1		fast
TB6MS	6-Month Treasury Bill: Secondary Market Rate (Percent)	1		fast
GS1	1-Year Treasury Constant Maturity Rate (Percent)	1		fast
GS10	10-Year Treasury Constant Maturity Rate (Percent)	1		fast
AAA	Moodys Seasoned Aaa Corporate Bond Yield (Percent)	1		fast
BAA	Moodys Seasoned Baa Corporate Bond Yield (Percent)	1		fast
BAA10YM	Moodys Seasoned Baa Corporate Bond Yield Rel. to Yield on 10-Year Treasury	1		fast
TB6M3Mx	6-Month Treasury Bill Minus 3-Month Treasury Bill, secondary market (Percent)	1		fast
GS1TB3Mx	1-Year Treasury Constant Maturity Minus 3-Month Treasury Bill, second market	1		fast
GS10TB3Mx	10-Year Treasury Constant Maturity Minus 3-Month Treasury Bill, second market	1		fast
CPF3MTB3Mx	3-Month Commercial Paper Minus 3-Month Treasury Bill, second market	1		fast
GS5	5-Year Treasury Constant Maturity Rate	1		fast
TB3SMFFM	3-Month Treasury Constant Maturity Minus Federal Funds Rate	1		fast
T5YFFM	5-Year Treasury Constant Maturity Minus Federal Funds Rate	1		fast
AAAFFM	Moodys Seasoned Aaa Corporate Bond Minus Federal Funds Rate	1		fast
M1REAL	Real M1 Money Stock	50		fast
M2REAL	Real M2 Money Stock	50		fast
BUSLOANSx	Real Commercial and Industrial Loans, All Commercial Banks	50		fast
CONSUMERx	Real Consumer Loans at All Commercial Banks	50		fast
NONREVSLx	Total Real Nonrevolving Credit Owned and Securitized, Outstanding	50		fast
REALLNx	Real Real Estate Loans, All Commercial Banks	50		fast
TOTALSLx	Total Consumer Credit Outstanding	50		fast
TOTRESNS	Total Reserves of Depository Institutions	50		fast
NONBORRES	Reserves Of Depository Institutions, Nonborrowed	7		fast
DTCOLNVHFNM	Consumer Motor Vehicle Loans Outstanding Owned by Finance Companies	50		fast
DTCTHFNM	Total Consumer Loans and Leases Outstanding Owned and Sec by Finance Comp.	50		fast
INVEST	Securities in Bank Credit at All Commercial Banks	50		fast
TABSHNOx	Real Total Assets of Households and Nonprofit Organizations	50		fast
EXSZUSx	Switzerland / U.S. Foreign Exchange Rate	50		fast
EXJPUSx	Japan / U.S. Foreign Exchange Rate	50		fast
EXUSUKx	U.S. / U.K. Foreign Exchange Rate	50		fast
EXCAUSx	Canada / U.S. Foreign Exchange Rate	50		fast
S.P.500	S&Ps Common Stock Price Index: Composite	5		fast
S.P..indust	S&Ps Common Stock Price Index: Industrials	50		fast
S.P.div.yield	S&Ps Composite Common Stock: Dividend Yield	1		fast

Note: Transformation codes (in Column Trans.): (1) no transformation, (5) $\Delta \log(x_t)$, (50) $\Delta \log(x_t)$ yoy-transformation, (7) $\Delta(x_t/x_{t-1} - 1.0)$